Mitotic chromosomes are compacted laterally by KIF4 and condensin and axially by topoisomerase IIα

Kumiko Samejima,[1] Itaru Samejima,[1] Paola Vagnarelli,[1] Hiromi Ogawa,[1] Giulia Vargiu,[1] David A. Kelly,[1] Flavia de Lima Alves,[1] Alastair Kerr,[1] Lydia C. Green,[2] Damien F. Hudson,[2] Shinya Ohta,[1] Carol A. Cooke,[5] Christine J. Farr,[3] Juri Rappsilber,[1,4] and William C. Earnshaw[1]

[1]Wellcome Trust Centre for Cell Biology, University of Edinburgh, King's Buildings, Edinburgh EH9 3JR, Scotland, UK
[2]Murdoch Childrens Research Institute, Royal Children's Hospital, Melbourne, Victoria 3052, Australia
[3]Department of Genetics, University of Cambridge, Cambridge CB2 3EH, England, UK
[4]Department of Biotechnology, Technische Universität Berlin, 13353 Berlin, Germany
[5]Neurology-Peripheral Nerve Division, Johns Hopkins University, Pathology-537, Baltimore, MD 21287

Mitotic chromosome formation involves a relatively minor condensation of the chromatin volume coupled with a dramatic reorganization into the characteristic "X" shape. Here we report results of a detailed morphological analysis, which revealed that chromokinesin KIF4 cooperated in a parallel pathway with condensin complexes to promote the lateral compaction of chromatid arms. In this analysis, KIF4 and condensin were mutually dependent for their dynamic localization on the chromatid axes. Depletion of either caused sister chromatids to expand and compromised the "intrinsic structure" of the chromosomes (defined in an in vitro assay), with loss of condensin showing stronger effects. Simultaneous depletion of KIF4 and condensin caused complete loss of chromosome morphology. In these experiments, topoisomerase IIα contributed to shaping mitotic chromosomes by promoting the shortening of the chromatid axes and apparently acting in opposition to the actions of KIF4 and condensins. These three proteins are major determinants in shaping the characteristic mitotic chromosome morphology.

Introduction

Mitotic chromosomes contain roughly equal amounts of DNA and histones, which comprise 60% of the protein present in isolated chromosomes (Ohta et al., 2010a,b). The remaining 40% of the protein mass consists of ∼4,000 nonhistone proteins (Ohta et al., 2010a). It is now accepted that nonhistone proteins have essential roles in organizing the higher-order structure of mitotic chromosomes. How they accomplish this is still poorly understood (Belmont, 2006; Marko, 2008; Moser and Swedlow, 2011; Ohta et al., 2011).

Laemmli and co-workers first suggested that nonhistone proteins of the "chromosome scaffold" fraction have an important role in mitotic chromosome structure (Adolph et al., 1977a,b). The first two scaffold proteins identified in purified chromosomes (Lewis and Laemmli, 1982) were topoisomerase IIα (topo IIα) and condensin core subunit SMC2 (Earnshaw et al., 1985; Gasser et al., 1986; Saitoh et al., 1994). Together with the other condensin subunits, these proteins were also major components of mitotic chromosomes assembled in vitro in *Xenopus* egg extracts (Hirano and Mitchison, 1994; Hirano et al., 1997). Later it was shown that animals and plants have two condensin complexes that share core subunits (SMC2 and SMC4) but differ in their auxiliary non-SMC subunits: with condensin I containing CAP-D2/G/H and condensin II CAP-D3/G2/H2 (Hirano et al., 1997; Ono et al., 2003). Mitotic chromosomes isolated from chicken DT40 cells used in the present study have ∼10× less condensin II than condensin I (Ohta et al., 2010a).

Correspondence to William C. Earnshaw: bill.earnshaw@ed.ac.uk; or Kumiko Samejima: kumiko.samejima@ed.ac.uk

L.C. Green's present address is Cancercentrum, Sahlgrenska Academy, Medicinaregatan 1G, plan 6, 41390 Göteborg, Sweden.

Abbreviations used in this paper: CAP, chromosome-associated polypeptide; IMS, intrinsic metaphase structure; RCA, regulator of chromosome architecture; SBP, streptavidin-binding peptide; $t_{1/2}$, half time; topo IIα, topoisomerase IIα.

The Rockefeller University Press $30.00
J. Cell Biol. Vol. 199 No. 5 755–770
www.jcb.org/cgi/doi/10.1083/jcb.201202155

Many studies have addressed the role of topo IIα and the condensin complexes in mitotic chromosome structure. The two localize on the chromatid axes (Earnshaw and Heck, 1985; Saitoh et al., 1994) in an alternating manner (Maeshima and Laemmli, 2003). Depletion of either topo IIα or condensin impairs chromosome organization and segregation (Holm et al., 1985; Uemura et al., 1987; Strunnikov et al., 1993; Saka et al., 1994; Bhat et al., 1996; Hirano et al., 1997; Hagstrom et al., 2002; Hudson et al., 2003, 2009; Vagnarelli et al., 2006; Csankovszki et al., 2009). If topo II is depleted in budding yeast, circular chromosomes accumulate positive supercoils in a condensin-dependent manner (Baxter et al., 2011). Interestingly, cells depleted of topo IIα or condensin can form mitotic chromosomes, albeit with an imperfect morphology (Steffensen et al., 2001; Chang et al., 2003; Hagstrom et al., 2002; Kaitna et al., 2002; Hudson et al., 2003; Carpenter and Porter, 2004; Sakaguchi and Kikuchi, 2004; Spence et al., 2007; Gonzalez et al., 2011). We therefore hypothesized that other uncharacterized scaffold components, possibly including the little-studied kinesin superfamily member KIF4, might also have important roles in mitotic chromosome structure in vertebrate cells.

KIF4 is a dimeric plus end–directed microtubule-based motor protein (Aizawa et al., 1992; Sekine et al., 1994; Oh et al., 2000; Lee et al., 2001; Samejima et al., 2008) also known as chromokinesin (Wang and Adler, 1995), CAP-D1 (chromosome associated polypeptide-D1; Hirano et al., 1997; MacCallum et al., 2002), Xklp-1 (*Xenopus* kinesin-like protein-1; Vernos et al., 1995), and KLP3A (*Drosophila* kinesin-like protein 3A; Williams et al., 1995). In cultured cells KIF4 is mainly nuclear during interphase, but relocates to the chromatid axes, spindle, spindle midzone, and midbody during mitosis (Vernos et al., 1995; Lee et al., 2001; Mazumdar et al., 2004).

Why would a motor protein that moves cargos along microtubules spend most of the cell cycle in the cell nucleus? During interphase, KIF4 appears to function in heterochromatin formation and the regulation of gene expression (Mazumdar et al., 2011). KIF4 has been shown to interact with condensin, DNA methyltransferase 3B, members of the NURD histone deacetylase complex, and PARP-1 (Geiman et al., 2004; Mazumdar et al., 2004, 2011; Midorikawa et al., 2006). During mitotic exit KIF4 functions together with PRC1 in formation of the central spindle and midbody (Kurasawa et al., 2004; Kwon et al., 2004; Castoldi and Vernos, 2006; Hu et al., 2011). However, KIF4's role on mitotic chromosomes remains poorly understood.

We have used conditional knockout chicken DT40 cell lines combined with RNAi knockdowns to investigate the functional relationships between KIF4, condensin, and topo IIα and their roles in establishing mitotic chromosome architecture. Our studies reveal that KIF4 and condensin work in parallel to promote mitotic chromosome morphology, acting in apparent opposition to topo IIα.

Results

We previously established a conditional knockout of KIF4 in chicken DT40 cells using a "promoter hijack" strategy in which a region of 6 kb upstream from the ATG was replaced with a tetracycline-repressible promoter (Samejima et al., 2008). When transcription from the modified KIF4 locus was switched off by adding doxycycline, KIF4 protein levels fell dramatically by 24 h later (Samejima et al., 2008). We use KIF4^{ON} to refer to those cells grown without doxycycline, and KIF4^{OFF} to refer to the cells grown with doxycycline for ≥24 h.

KIF4^{OFF} DT40 cells exhibited multiple mitotic defects affecting both chromosome structure and cytokinesis. However, in contrast with results of KIF4 RNAi in HeLa cells (Mazumdar et al., 2004), spindles appeared largely normal in early mitosis and the cells did not accumulate at prometaphase.

KIF4 preferentially colocalizes with SMC2 on chromatid axes

In DT40 cells, KIF4 localizes on the chromatid axes in a punctate pattern similar to condensin and topo IIα (Fig. 1 A; Earnshaw and Heck, 1985; Saitoh et al., 1994). This distribution was seen previously (Mazumdar et al., 2004), and it was suggested that KIF4 acts as a spacer for condensin complexes on chromosomes (Mazumdar and Misteli, 2005).

All three proteins exhibit significant overlap. To quantitate the extent of their colocalization, we generated coordinated datasets of fluorescence intensities at each pixel from 10 chromosome spreads and calculated Pearson correlation coefficients for all pairwise combinations. In this analysis, total positive correlation appears as 1, total negative correlation as −1, and no correlation as 0. The combination of KIF4 vs. SMC2 showed the highest correlation (R = 0.51), with lower values determined for topo IIα vs. SMC2 (R = 0.39) and KIF4 vs. topo IIα (R = 0.37; Fig. 1 A). Thus, KIF4 on chromatid axes is more closely correlated with SMC2 than topo IIα.

Interdependence of KIF4, condensin, and topo IIα for localization on chromosomes

We used conditional knockout cell lines expressing labeled SMC2 or condensin auxiliary subunits in the absence of the corresponding endogenous protein to examine the interdependencies of condensin and KIF4 for localization on mitotic chromosomes. Total condensin was visualized using SMC2^{OFF} cells expressing SMC2-GFP-STS (see Materials and methods and Fig. 1, B–E). Condensin I was visualized using CAP-H^{OFF} cells expressing CAP-H-GFP-TrAP (Samejima et al., 2008; Green et al., 2012). Condensin II was visualized using CAP-D3^{OFF} cells expressing CAP-D3-GFP-TrAP (Green et al., 2012). All three tagged proteins are functional and rescue viability in the absence of their endogenous counterparts. KIF4 was depleted by transfection with KIF4 siRNA. Quantification of protein levels in the RNAi experiments is shown in Fig. S1 A.

Total condensin was relatively enriched at kinetochores after KIF4 depletion: residual SMC2 spots colocalized with kinetochore marker CENP-T (Fig. 1, B–E). This apparent enrichment is due to preferential loss of condensin from the chromosome arms. The SMC2-GFP signal was reduced by 56% on chromatid axes after KIF4 depletion, but only by half as much (32%) at kinetochores (Fig. 1 D).

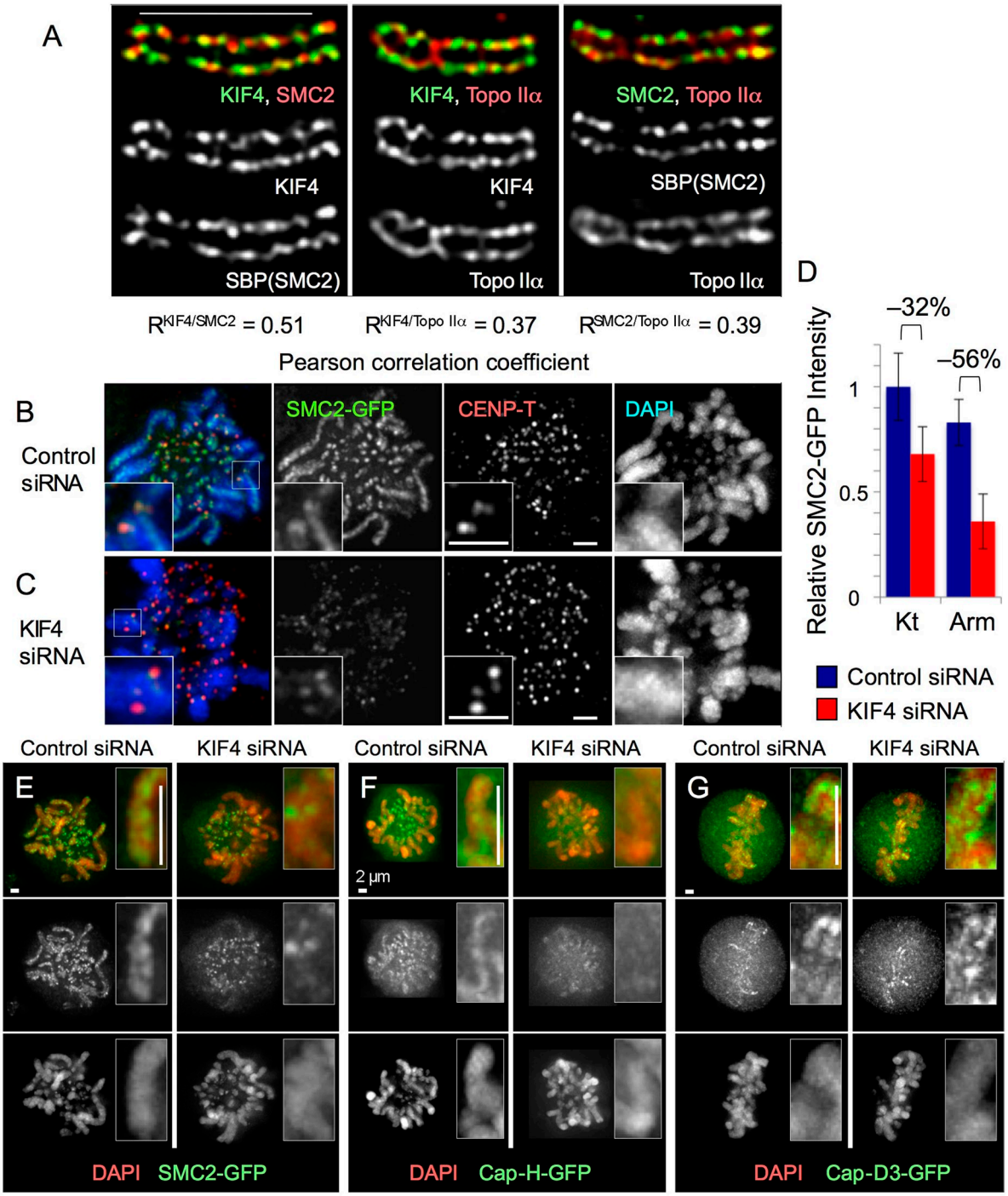

Figure 1. **KIF4 partially colocalizes with SMC2 and topo IIα and affects condensin localization on the chromosome axis.** (A) $SMC2^{OFF}$ cells expressing SMC2-TrAP were stained with guinea pig anti-topo IIα, mouse anti-SBP, and rabbit anti-KIF4 plus DAPI for the DNA. Bar, 5 μm. (B and C) Asynchronously growing $SMC2^{OFF}$:SMC2-GFP-STS cells were transfected with either control or KIF4 siRNA oligos. After 20–24 h, these cells were fixed in PFA/PBS and stained by anti–CENP-T antibody and DAPI. Bars, 2 μm. (D) Quantification of B and C. Intensity of SMC2-GFP signal was measured at 5 kinetochores (Kt), 5 chromosome arms (Arm), and 5 areas in the cytosol in each of 20 cells. (E–G) Asynchronously growing $SMC2^{OFF}$:SMC2-GFP-STS cells (E), CAP-H^{OFF}: CAP-H-GFP-TrAP cells (F), or CAP-$D3^{OFF}$:CAP-D3-GFP-TrAP cells (G) were treated as in B and C and stained with DAPI. Bars, 2 μm.

After KIF4 depletion, the total signal of condensin I was reduced along the chromatid axes (Fig. 1 F). In contrast, condensin II localization was much less affected by KIF4 depletion (Fig. 1 G). This observation that the chromosomal distribution of condensin I is more altered than condensin II after KIF4 depletion is consistent with the results of our proteomics experiments (see subsequent section).

We also examined the localization interdependencies of endogenous condensin, KIF4, and topo IIα on chromosomes (Fig. 2). As observed previously, KIF4 is required for SMC2

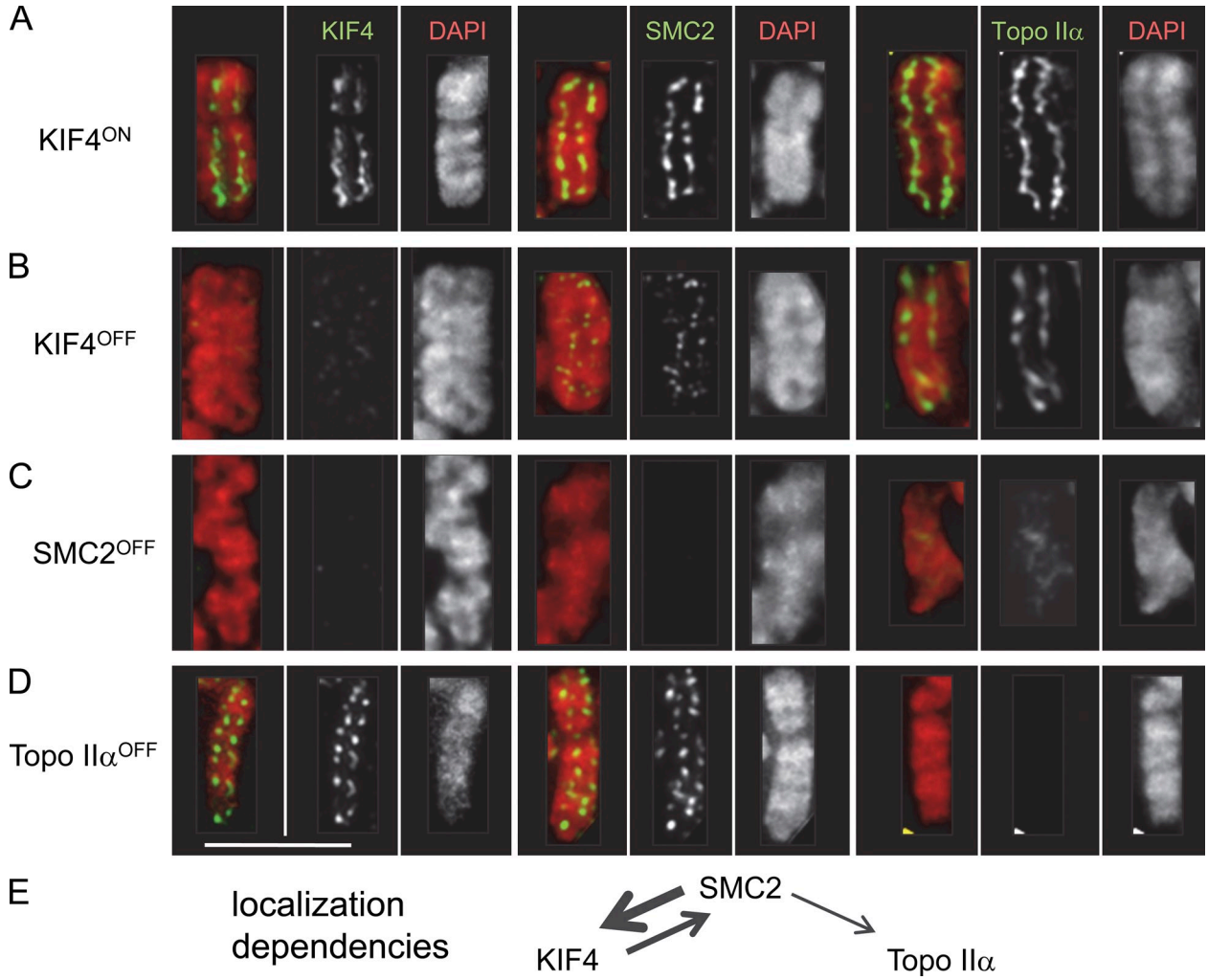

Figure 2. **Interdependence of chromosome axis localization for KIF4 and SMC2.** (A and B) KIF4$^{ON/OFF}$, (C) SMC2^{OFF}, and (D) Topo IIα^{OFF} cells were stained with anti-KIF4, anti-SMC2, or anti-topo IIα antibodies plus DAPI. (E) Summary of localization dependencies. Bar, 5 µm.

(e.g., total condensin I plus II) to localize normally on chromatid axes (Mazumdar et al., 2004). In indirect immunofluorescence of KIF4^{OFF} chromosomes, the SMC2 signal was reduced and dispersed on the chromosomes (Fig. 2 B).

In reciprocal experiments, endogenous KIF4 protein levels were strongly reduced on chromosomes of SMC2^{OFF} cells and the remaining protein was distributed diffusely (Fig. 2 C). Similarly, GFP-KIF4^{wt}, which was clearly recognized on chromatid axes in control cells fixed in hypotonic solution (paraformaldehyde [PFA]/75 mM KCl), appeared very faint and diffuse on chromosomes after SMC2 depletion (Fig. S1 C). In control cells fixed under nonhypotonic conditions (PFA/PBS), GFP-KIF4^{wt} was seen both on chromosomes and in the cytosol. The chromosomal signal was strongly reduced after SMC2 depletion. For a summary of the cell pretreatment and chromosome fixation conditions used in all figures, see Table S1.

Topo IIα was distributed diffusely and only faintly detectable on SMC2^{OFF} chromosomes (Fig. 2 C; see also Hudson et al., 2003). Topo IIα localization was normal on KIF4-depleted chromosomes, but the level of immunolabeling was slightly reduced (Fig. 2, A and B). The distribution of both KIF4 and SMC2 appeared essentially normal on topo IIα–depleted chromosomes (Fig. 2 D).

We conclude that both KIF4 and topo IIα depend on SMC2 for their localization on the chromatid axis and that SMC2 exhibits a reciprocal dependency on KIF4 for localization on the chromatid axes (Fig. 2 E).

KIF4 is highly dynamic on mitotic chromosomes

To measure KIF4 dynamics on chromosomes we performed FRAP analysis on KIF4^{OFF} cells stably expressing GFP-KIF4^{wt} in metaphase using the proteasome inhibitor MG132. The tagged KIF4 rescues life and is the only KIF4 expressed in these cells. We photobleached a 1-µm-diameter circle on the chromosomes and measured the GFP fluorescence recovery every 0.4 s thereafter. The mean half-time for GFP-KIF4 recovery ($t_{1/2}$) was 2.3 s, similar to that published for topo IIα (Christensen et al., 2002; Tavormina et al., 2002) with an immobile fraction of 13% (Fig. 3). In contrast, the half time for recovery of condensin I is ~50× slower (Gerlich et al., 2006; Oliveira et al., 2007; unpublished data). The mobility of condensin I was essentially unaffected by depletion of KIF4 (unpublished data).

Although KIF4 preferentially localizes on chromatid axes, a substantial amount of the protein is also present in the cytosol

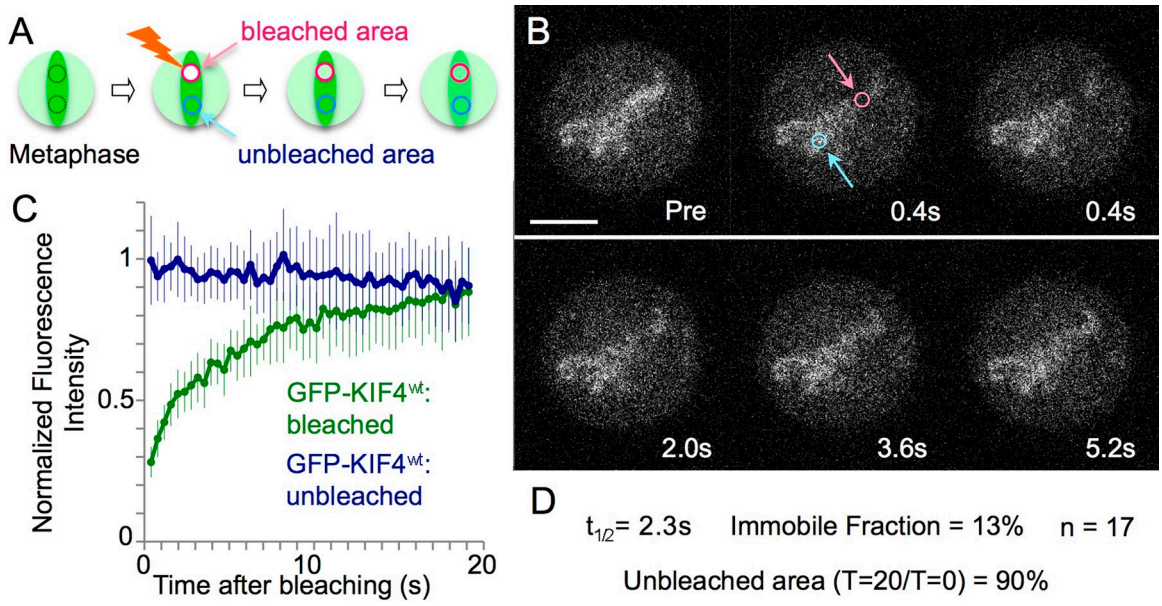

Figure 3. **KIF4 is highly mobile between chromosomes and cytosol.** (A) Schematic presentation of the FRAP experiment. (B) Stills from the FRAP experiment of GFP-KIF4^{wt} expressed in KIF4^{OFF} cells blocked in metaphase using MG132. Bar, 5 µm. (C and D) FRAP analysis. Error bars show SD.

and on the spindle. To determine if KIF4 shuttles between its various locations during mitosis, we next bleached the entire metaphase plate (Fig. S2, A and A′). This yielded essentially identical parameters with a $t_{1/2}$ of 2.1 s and immobile fraction of 15%. We also bleached the entire cell with the exception of half of the metaphase plate. We again observed a rapid ($t_{1/2}$ of 1.4 s) recovery of 70% of the fluorescence (Fig. S2, B and B′). The lowered recovery presumably reflects limiting amounts of remaining fluorescent KIF4.

We conclude that with the exception of a small immobile fraction that may be associated with the chromosome scaffold, most chromosomal KIF4 is highly dynamic with rapid exchange between chromosomal and cytosolic pools.

Effects of KIF4 depletion on the proteome of mitotic chromosomes

Quantitative SILAC mass spectrometry analysis of chromosomes isolated from wild-type and KIF4^{OFF} cells revealed that isolated KIF4^{OFF} mitotic chromosomes retain 6% of the wild-type level of KIF4 (Fig. 4 C). This proteomic analysis failed to reveal any other protein whose level of depletion matched that of KIF4 on the mutant chromosomes. Such a corresponding degree of depletion would be expected for proteins that form obligate complexes with KIF4 on chromosomes (Ohta et al., 2010a). In this analysis, complexes typically behave as integral units with all subunits showing an essentially identical response (Fig. 4, C and D).

Condensin I, macroH2A.2, HMGN1 and HMGN2, and DEK were all significantly decreased in chromosomes depleted of KIF4 (Fig. 4, A and C). KIF4 has previously been reported to bind to condensin (Geiman et al., 2004; Mazumdar et al., 2004). Interestingly, condensin II subunits were slightly less affected by KIF4 depletion. This is consistent with the different effects of KIF4 depletion on the localization of condensin I and II on chromosome arms (Fig. 1) and with the morphology of KIF4-depleted chromosomes (Fig. S3 C). An exception is CAP-D3, which behaves divergently from all other condensin subunits in both the KIF4 and SMC2 knockouts. Our proteomics data suggest that this protein might be in another complex in addition to condensin II.

To further examine the dependencies between KIF4 and condensin for association with chromosomes, we also reanalyzed data from our previously published proteomic analysis of mitotic chromosomes depleted of SMC2 (Ohta et al., 2010a). In the absence of SMC2, all condensin I subunits and most condensin II subunits were reduced to a similar degree on isolated mitotic chromosomes (Fig. 4 B). After the condensin subunits, KIF4 is the next most strongly affected chromosomal protein in SMC2-depleted chromosomes, being reduced to approximately half of its wild-type level (Fig. 4 B). In contrast, topo IIα and topo IIβ were little affected in either the KIF4- or SMC2-depleted cells (Fig. 4, A–C).

KIF4 can bind and negatively regulate the activity of PARP-1 (Midorikawa et al., 2006; Mazumdar et al., 2011), one of the most abundant chromosomal nonhistone proteins (Ohta et al., 2010a). PARP1 levels increase after KIF4 depletion (Fig. 4 C), raising the possibility that PARP1 enzymatic activity may be increased on KIF4-depleted chromosomes. Levels of the KIF4 binding partner Asf1 (Mazumdar et al., 2011) were slightly increased, whereas PRC1 (Kurasawa et al., 2004) was slightly decreased on KIF4-depleted chromosomes. Most components of the chromosome periphery were increased on KIF4-depleted chromosomes. This likely reflects an increase in chromosome surface area during the hypotonic treatment and lysis of cells during the chromosome isolation protocol (Fig. 5 A).

Kinetochore protein complexes showed a variety of responses to the absence of KIF4 (Fig. 4 D). The chromosomal passenger complex (CPC) and RZZ complex were slightly

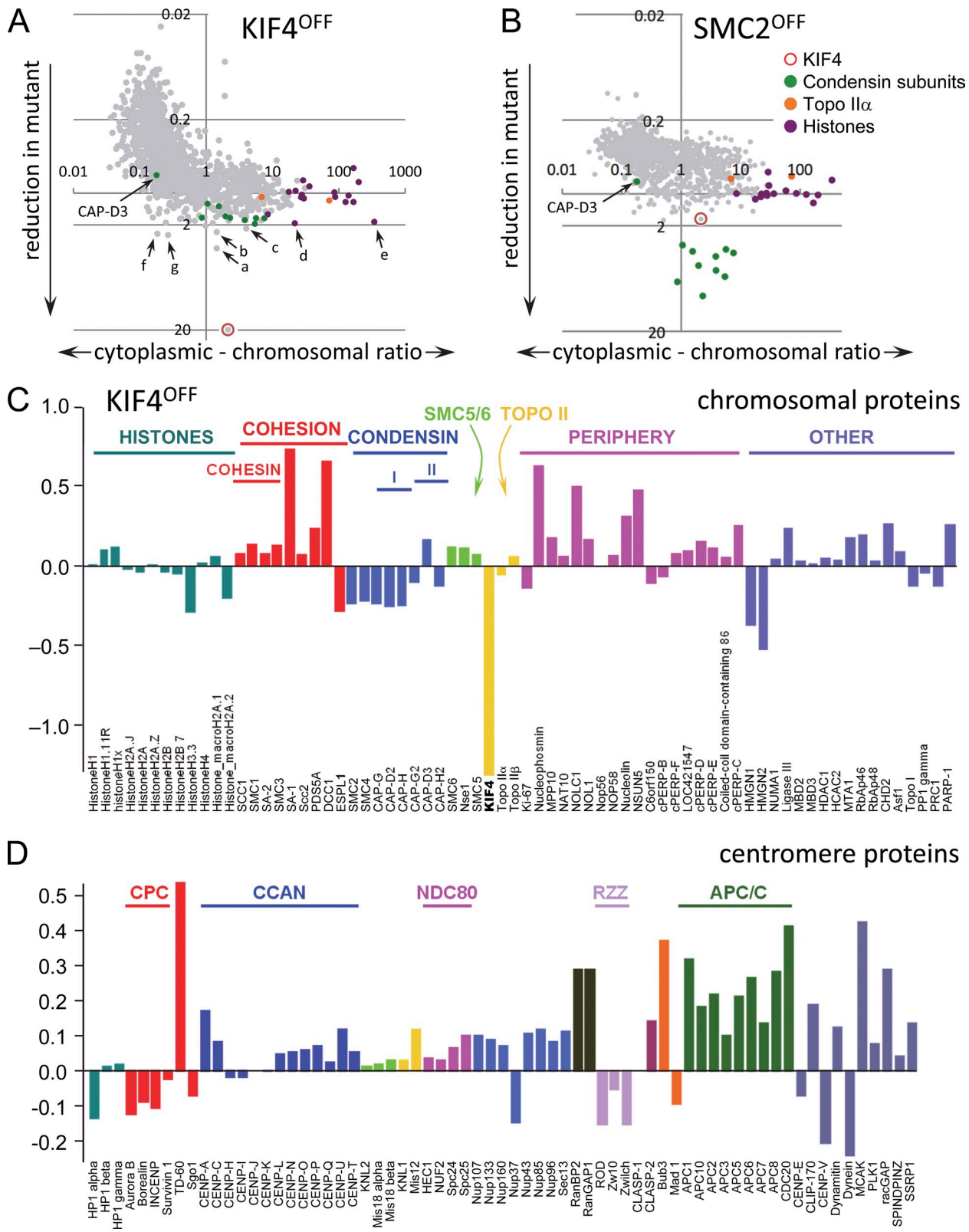

Figure 4. **Proteomic analysis of KIF4^{OFF} and SMC2^{OFF} isolated chromosomes.** (A) Dependency of proteins on KIF4 for their association with mitotic chromosomes. Proteins reduced in mitotic chromosomes isolated from KIF4^{OFF} cells (relative to those on chromosomes isolated from wild-type cells) appear lower on the y axis. Proteins enriched on chromosomes relative to cytoplasm appear to the right on the x axis. This is Classifier II of Ohta et al. (2010a), and uses values from those experiments. Proteins most strongly depleted in this experiment include the chromatin proteins HMGN2 (a), HMGN1 (b), DEK (c), H3.3 (d), and H1.03 (e) and cytoplasmic proteins cytidine deaminase (f) and CKS1B (g). (B) Similar analysis of SMC2 dependency based on the published proteomic analysis of isolated chromosomes from wild-type and SMC2^{OFF} cells (Ohta et al., 2010a). (C and D) Diagrams showing the dependency of selected chromosomal (C) and centromeric (D) proteins for their association with isolated mitotic chromosomes in the presence and absence of KIF4. Bars point downward when the corresponding protein is decreased in KIF4^{OFF} chromosomes.

decreased, whereas RanBP2/RanGAP1 and the APC/C were significantly increased. No systematic change was seen in the CCAN, where CENP-A and the CENP-O complex were increased, but other components showed no change. This pattern of changes in centromere proteins is consistent with the observation that chromosome alignment and movements are normal in KIF4^{OFF} cells (unpublished data).

Collectively, the proteomics experiments confirm a link between condensin and KIF4 for stable association with mitotic chromosomes, consistent with the localization data of Fig. 2. In contrast, neither protein is required for topo IIα to associate with mitotic chromosomes (though condensin is required for its correct axial localization).

KIF4^{OFF} chromosomes are shorter and wider than normal with compromised structural integrity

To define the effects of KIF4 depletion on mitotic chromosome morphology, asynchronously growing KIF4$^{ON/OFF}$ cells were treated with hypotonic buffer and mitotic chromosomes examined after DAPI staining of the DNA. The arms of KIF4^{OFF} chromosomes appeared wider and less sharply defined compared with KIF4^{ON} chromosomes (Fig. 5 A).

Because chromosome length and width varies significantly depending on the mitotic stage, we carefully measured chromosome dimensions in KIF4$^{ON/OFF}$ cultures after release from a G2 block with the CDK inhibitor R03306. Cells were attached to slides, treated with 75 mM KCl for 5 min, fixed with cold methanol/acetic acid, stained with DAPI, and the length and width of the third-longest chromosome were measured (Fig. S3 C). KIF4^{OFF} chromosomes tended to be shorter and slightly wider than KIF4^{ON} chromosomes. Thus, chromosomes depleted of KIF4 more closely resemble those depleted of condensin I rather than condensin II (Green et al., 2012).

We measured the distance between sister kinetochores to assess KIF4's role in compaction of the centromeric heterochromatin. In cultures incubated with the microtubule-depolymerizing drug colcemid (no spindle tension), the inter-kinetochore distance was similar in prometaphase KIF4^{ON} and KIF4^{OFF} cells (Fig. 5 C, Tension −). Thus, although KIF4 has a reported role in the formation of interphase heterochromatin (Mazumdar et al., 2011), it is not required to compact inner centromere heterochromatin during mitosis. Importantly, these measurements were made on chromosomes from cells kept under physiological conditions until after fixation (Table S1).

When microtubules attach and sister kinetochores come under tension from opposite spindle poles, the distance between them reflects the stiffness (compliance) of the centromeric heterochromatin (Bouck and Bloom, 2007; Ribeiro et al., 2009; Jaqaman et al., 2010). This "tense" inter-kinetochore distance in KIF4^{OFF} cells was 25% greater than that in KIF4^{ON} cells held in metaphase by MG132 (Fig. 5 C, Tension +). This suggests that KIF4, like condensin (Ribeiro et al., 2009), helps to establish the proper compliance of centromeric heterochromatin. Interestingly, loss of topo IIα seems to stiffen the centromeric chromatin "spring" (Fig. 5 F; Fig. S3 B; Spence et al., 2007; Ribeiro et al., 2009).

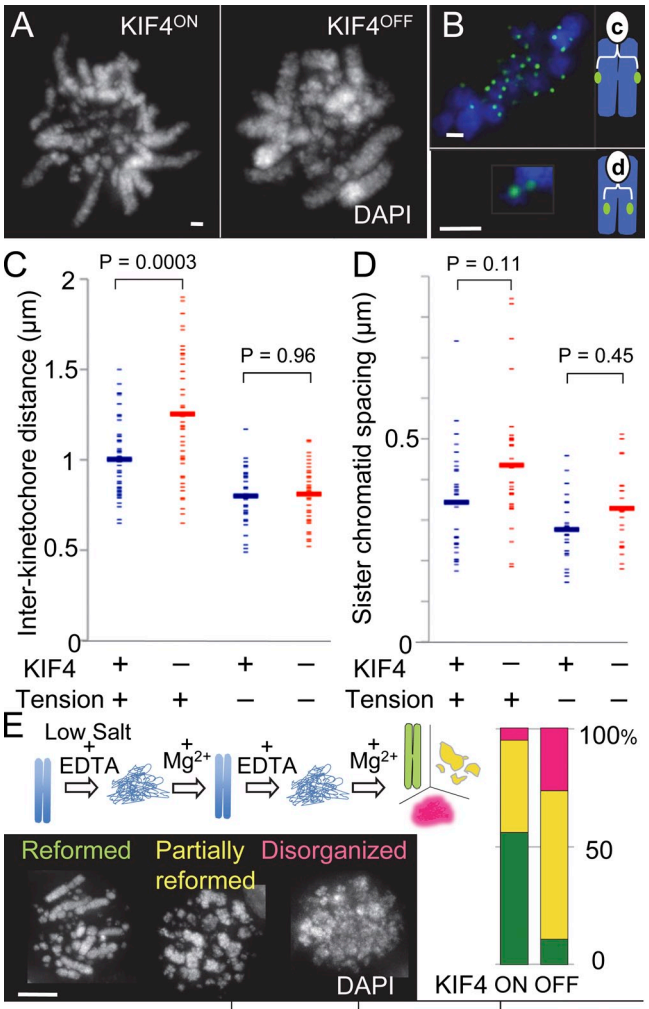

F

	KIF4^{OFF}	SMC2^{OFF}	Topo IIα^{OFF}
Chromosome width	Expanded	Highly expanded	Reduced
Inter-Kt Distance (+ tension)	125%	140%*	95%
Structural integrity	Reduced	Lost	Retained

Figure 5. **Architecture of chromosomes is compromised after KIF4 depletion.** (A) KIF4$^{ON/OFF}$ prometaphase chromosomes. Asynchronously growing cells were subjected to hypotonic treatment (75 mM KCl for 5 min), fixed in 4% PFA in the same buffer, and stained with DAPI. Bar, 1 µm. (B) KIF4$^{ON/OFF}$ cells with a CENP-H-GFP knock-in (top) and or integrated LacO array and expressing LacI-GFP (bottom) were fixed and stained as in A. Bars, 1 µm. (C) Interkinetochore distance. CENP-H-GFP knock-in cells from B (top) were treated either with MG132 (tension +) or with colcemid (tension −) for 3 h and fixed in 4% PFA/PBS. n = 50 from 10 cells. Wider bars represent the mean distance. The difference is statistically significant (D = 0.42, P = 0.0003; KS test) only in the presence of tension. D = 0.1, P = 0.96 (Tension −). (D) Sister chromatid spacing. KIF4$^{ON/OFF}$ LacO–bearing cells expressing LacI-GFP (B, bottom) were treated as in C. n > 20. Differences were not statistically significant: D = 0.31, P = 0.11 (Tension +, KS test); D = 0.25, P = 0.45 (Tension −). Data are shown from a single representative experiment out of two repeats. (E) Intrinsic metaphase structure assay of KIF4$^{ON/OFF}$ chromosomes as described in the text. 100 cells were scored per sample. Bar, 5 µm. Data are shown from a single representative experiment out of two repeats. (F) Summary of chromosomal phenotypes exhibited after depletion of KIF4, SMC2, or Topo IIα. *, interkinetochore distance of SMC2$^{ON/OFF}$ cells (Vagnarelli et al., 2006).

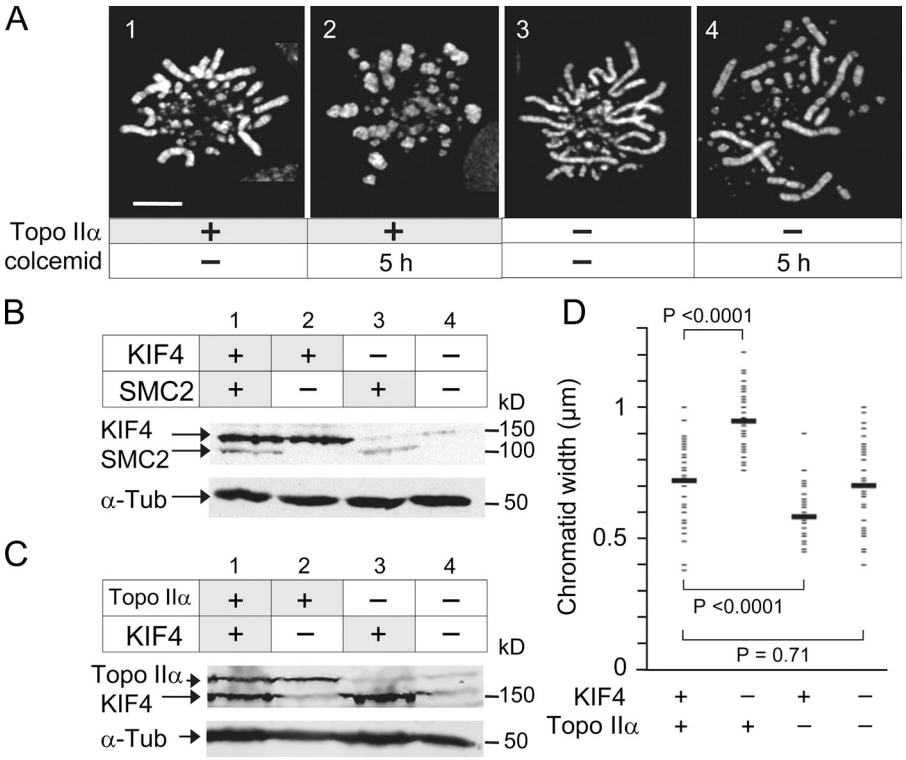

Figure 6. **Topo IIα is required for axial shortening during mitosis.** (A) Cells treated with Dox for 43 h to induce expression of a Topo IIα–specific shRNA (1 and 3) were swollen in 75 mM KCl, fixed in methanol acetic acid, and stained by DAPI. This was done plus or minus addition of colcemid for a further 5 h (2 and 4). Bar, 5 µm. (B) For the double condensin/KIF4 knockdown, $SMC2^{ON/OFF}$ cells (lane 2) were transfected with KIF4 siRNA oligonucleotides (lane 3), with addition of doxycycline (30 h) resulting in the double depletion (lane 4). α-Tubulin was used as a loading control. (C) For the double condensin/topo IIα knockdown, topo IIα inducible shRNA cells were treated with KIF4 siRNA oligos (lane 2), with addition of doxycycline (48 h) resulting in the double depletion (lane 4). α-Tubulin was used as a loading control. (D) Chromosome width of cells in C was measured at randomly selected noncentromeric positions. The mean is shown by a heavy bar. D- and P-values were obtained by: The difference is statistically significant between control and KIF4-depleted (D = 0.64, P < 0.0001; KS test) or Topo IIα–depleted (D = 0.52, P < 0.0001 cells), but not double-depleted (D = 0.14, P = 0.71) cells. Data are shown from a single representative experiment out of two repeats.

We also measured the distance between lacO loci on sister chromatid arms in order to investigate whether KIF4 has a role in compaction and cohesion of noncentromeric chromatin. This distance was ∼10% greater in $KIF4^{OFF}$ cells irrespective of the presence or absence of spindle tension. KIF4 may contribute either to lateral compaction of the chromatid arms or to sister chromatid cohesion (Fig. 5 D).

We next assessed the structural integrity of $KIF4^{OFF}$ chromosomes using the intrinsic metaphase structure (IMS) assay (Fig. 5 E) previously developed for analysis of chromosomes depleted of SMC2 and topo II (Hudson et al., 2003; Spence et al., 2007). Chromosomes of cells blocked in mitosis by colcemid were subjected to two cycles of expansion and refolding in TEEN buffer (1 mM triethanolamine:HCl, pH 8.5, 0.2 mM NaEDTA, and 25 mM NaCl). In this buffer, the negative charge of the DNA is not fully neutralized and chromosomes swell into amorphous masses lacking any higher-order chromatin structure beyond the 10-nm fiber (Earnshaw and Laemmli, 1983). Addition of divalent cations restores the chromosome morphology (Earnshaw and Laemmli, 1983).

After two rounds of swelling and shrinking, 56% of $KIF4^{ON}$ chromosomes reformed a normal chromosome morphology (Fig. 5 E, green bar; Fig. S3 A). This number fell to 11% for $KIF4^{OFF}$ chromosomes (mean of four experiments). These numbers resemble the effect seen when cells are depleted of condensin ($SMC2^{OFF}$), though condensin depletion results in a stronger phenotype (Fig. S3 A). Depletion of topo IIα had no effect on the intrinsic structure of mitotic chromosomes (Fig. S3 A; Spence et al., 2007).

We conclude that KIF4, like condensin, contributes to the "structural integrity" of mitotic chromosomes and is required for proper mitotic chromosome architecture.

Topo IIα is required to shorten chromatid axes during mitotic chromosome formation

To determine whether topo IIα is involved in shaping mitotic chromosomes, we exploited the fact that chromosomes continue to shorten throughout mitosis (Mora-Bermúdez et al., 2007). If cells are held for prolonged periods in mitosis with colcemid, the chromosomes adopt a characteristic stubby appearance (Fig. 6 A, panels 1 and 2). In the absence of colcemid, chromatids of topo IIα–depleted chromosomes were longer and thinner than wild type (Fig. 6 A, panels 1 and 3), as observed previously (Sakaguchi and Kikuchi, 2004; Spence et al., 2007). Remarkably, if topo IIα–depleted cells were held in mitosis with colcemid, the chromatids did not shorten further (Fig. 6 A, panel 4). This clearly demonstrated a specific requirement for topo IIα in shaping mitotic chromosomes by axial shortening during mitosis.

KIF4 and condensin act in parallel pathways antagonized by topo IIα to shape mitotic chromosomes

The spatial and functional relationships between KIF4 and condensin on mitotic chromosomes demonstrated in previous sections could be explained if KIF4 and condensin work in a common pathway. In that case, cells doubly depleted of condensin and KIF4 would be expected to exhibit defects similar to those observed in cells depleted of condensin alone. To test this hypothesis, single or double depletion of KIF4 and SMC2 was achieved by performing siRNA knockdowns on conditional knockout cells. As a control, we also performed double depletions of SMC2 with CAP-H (condensin I subunit) or CAP-D3 (condensin II subunit). In parallel experiments, we also determined the results of simultaneously knocking down the expression of topo IIα and KIF4 as well as the triple depletion

(SMC2, topo IIα, and KIF4). The efficacy of the double knockdowns is shown in Fig. 6 (B and C), with a quantitative analysis of residual protein levels in Fig. S1 B. Chromosome structure was assessed in chromosome spreads stained with DAPI either with or without hypotonic treatment of cells before cold methanol/acetic acid fixation (Fig. 7, A and B). We also quantitated the lateral compaction of chromosome arms by measuring the width of chromatids fixed in physiological buffer and stained with DAPI (Fig. 6 D).

Double depletion of KIF4 and SMC2 yielded a phenotype much stronger than that seen with either single depletion: chromosomes doubly depleted of KIF4 and SMC2 were highly disorganized. The chromatid width was variable and chromosome outlines were poorly defined (Fig. 7, A and B, compare panels 10 and 8, respectively, with panel 4). Although we could not provide a meaningful measure of chromatid width for this experimental pair, we were able to measure the sister chromatid spacing with or without tension. The latter clearly showed an additive effect of the double depletion (Fig. S4 C). In contrast, double depletion of SMC2 and CAP-H or CAP-D3 yielded essentially the same phenotype as single depletion of SMC2 (Fig. 7, panels 2, 5, 6, 8, 11, and 12). This argues against the possibility that the synergistic effect of double depletion of KIF4 and SMC2 was due to further loss of residual condensin from chromosomes after KIF4 depletion.

Remarkably, double depletion of KIF4 or SMC2 with topo IIα either partly or completely rescued the chromosome morphologies seen with single depletions. Chromosomes doubly depleted of KIF4 and topo IIα were almost indistinguishable from wild type (Fig. 6 D; Fig. 7 B, panels 5, 6, and 10). Similarly, chromosomes from cells doubly depleted of SMC2 and topo IIα were significantly less expanded and had sharper outlines than chromosomes depleted only of SMC2 (Fig. 7 B, compare panels 7 and 11). A particularly striking result was seen when we depleted all three proteins from DT40 cells. Although the KIF4/SMC2 double depletion resulted in a near complete loss of mitotic chromosome architecture (Fig. 7 B, panel 8), the additional depletion of topo IIα appeared to substantially rescue the chromosome morphology (Fig. 7 B, panel 12). Triply depleted chromosomes were variable in appearance, but overall appeared to be more compact and to have a more clearly defined outline than chromosomes double depleted for KIF4 and SMC2 (Fig. 7 B compare panels 8 and 12). Together, these results suggest that KIF4 and SMC2 act in parallel or additive pathways to shape mitotic chromosomes, with topo IIα acting in opposition.

The motor domain is required for KIF4's chromosomal functions

The N-terminal KIF4 motor domain (Gg aa 23–340) is followed by a long coiled-coil region and C-terminal globular domain (Fig. 8 A). Chromatin binding by KIF4 requires a central leucine-zipper region (aa 753–797) and a C-terminal cysteine-rich region (Gg aa 1083–1121; Wu et al., 2008). The C-terminal region (Mm aa 859–1236) is sufficient to perform the functions of KIF4 in heterochromatin formation in mouse embryonic stem cells (Mazumdar et al., 2011).

To examine the effects of KIF4 domains on mitotic chromosome structure, we constructed GFP fusion proteins with full-length, plus N- or C-terminal truncations of KIF4. Localization of these chimeric proteins was tested by transient transfection in $KIF4^{OFF}$ cells (i.e., in the absence of endogenous KIF4; Fig. 8 A). GFP-$KIF4^{1–1226}$ and GFP-$KIF4^{510–1226}$ both localized on mitotic chromosomes. In contrast, GFP-$KIF4^{920–1226}$, which lacks the central coiled-coil region, was diffuse in mitotic cells (Fig. S4 B), as were all truncations lacking the C-terminal domain. Thus, KIF4 binding to mitotic chromosomes requires both the central coiled-coil region and the C-terminal domain, but not the motor domain (Wu et al., 2008).

For more detailed mechanistic analysis, we established stable $KIF4^{ON/OFF}$ cell lines in which GFP-$KIF4^{wt}$ and GFP-$KIF4^{510–1226}$ were expressed at near endogenous levels (Fig. S4 A). The localization of GFP-$KIF4^{510–1226}$ along the chromatid axis was slightly disorganized after switching off endogenous KIF4 expression, whereas the distribution of GFP-$KIF4^{wt}$ appeared normal (Fig. 8 B). Furthermore, cells expressing GFP-$KIF4^{510–1226}$ as the sole form of KIF4 had chromatids that were expanded relative to those expressing GFP-$KIF4^{wt}$ (Fig. 8 B).

To test if GFP-$KIF4^{510–1226}$ lacking the kinesin motor domain could restore the compliance of centromeric chromatin, we measured the inter-kinetochore distance under tension, using an anti–CENP-T antibody to visualize kinetochores in cells lacking endogenous KIF4 (Fig. 8 C). As shown above (Fig. 5, C and F), the inter-kinetochore distance was 32% wider in $KIF4^{OFF}$ cells than in $KIF4^{ON}$ cells. Expression of GFP-$KIF4^{WT}$ rescued this phenotype (Fig. 8 C). In contrast, the inter-kinetochore distance in $KIF4^{OFF}$ cells expressing GFP-$KIF4^{510–1226}$ was 21% wider than that in $KIF4^{ON}$ cells. Thus the normal compliance of centromeric heterochromatin was not restored by GFP-$KIF4^{510–1226}$.

As shown above, loss of KIF4 compromises the structural integrity of chromosomes (Fig. 5 E). The IMS assay revealed that although expression of GFP-$KIF4^{WT}$ fully rescued chromosome integrity, expression of GFP-$KIF4^{510–1226}$ could not (Fig. 8 D).

In summary, KIF4 utilizes its stalk and C-terminal tail regions to target to mitotic chromosomes, but additionally requires its N-terminal motor domain to fully execute its chromosomal functions.

Discussion

Three abundant chromosome scaffold proteins—condensin, the chromokinesin KIF4, and DNA topoisomerase IIα—act together to shape mitotic chromosomes. KIF4 and condensin are required both for the proper compliance (stiffness) of centromeric heterochromatin and for establishment of the "intrinsic metaphase structure" of the chromosomes. Topo IIα is required for normal shortening of the chromatid arms during mitosis.

The "intrinsic metaphase structure" is defined by an assay in which chromosomes are unfolded and refolded by altering the ionic composition of the medium. Exactly what this means biologically is not known; however, this assay almost certainly

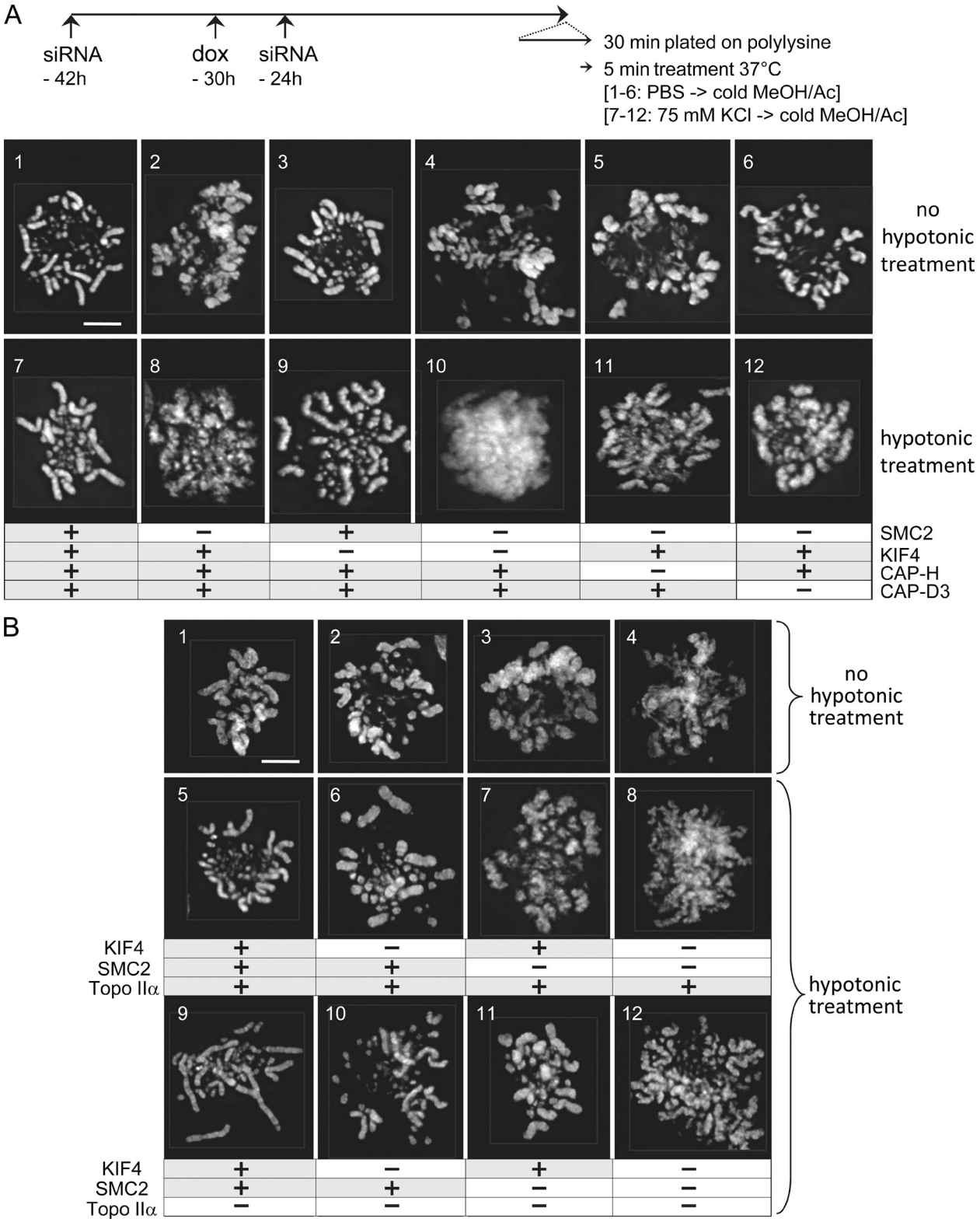

Figure 7. **KIF4 and SMC2 act in parallel to shape mitotic chromosomes and are opposed by Topo IIα.** (A) SMC2$^{ON/OFF}$ cells treated as shown were washed in either PBS or 75 mM KCl and fixed in methanol/acetic acid. (B) SMC2$^{ON/OFF}$ cells were transfected with either control or KIF4 or Topo IIα siRNA as in Fig. 6, B–D. Simultaneous transfection of the SMC2$^{ON/OFF}$ cells with KIF4 and Topo IIα siRNA oligos gave the triple knockout. Cells were washed in PBS or 75 mM KCl (hypotonic treatment), fixed in methanol acetic acid, and stained with DAPI. Bars, 5 µm.

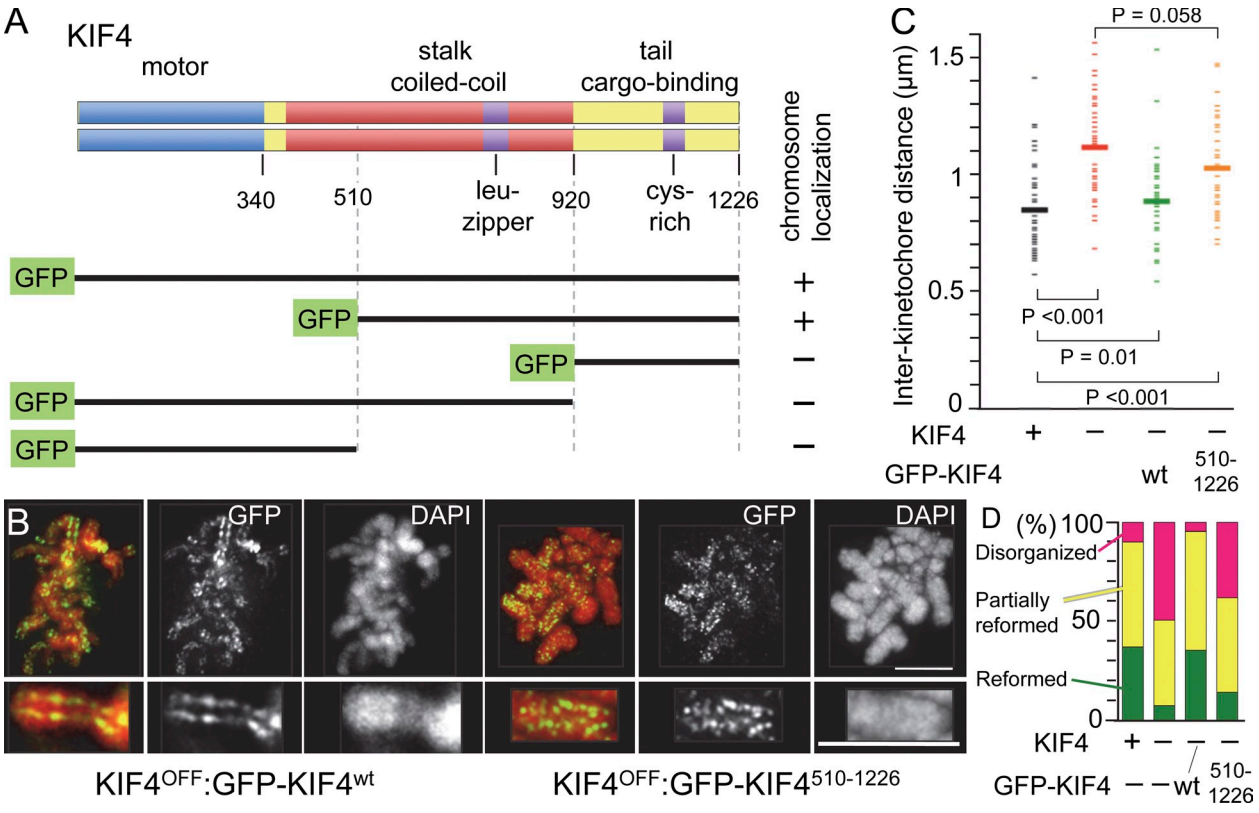

Figure 8. **KIF4 motor domain is required for its chromosomal functions.** (A) Schematic representation of KIF4 and the fragments expressed in KIF4^{OFF} cells. Right, chromosome axis localization is shown as + or − for each GFP fusion protein. (B) KIF4^{OFF} cells expressing GFP-KIF4^{wt} or GFP-KIF4$^{520\text{-}1226}$ were treated with 75 mM KCl, fixed in PFA/75 mM KCl, and stained with DAPI. Bars, 5 μm. (C) Interkinetochore distance in the presence of tension. KIF4$^{ON/OFF}$ cells or KIF4^{OFF} cells expressing GFP-KIF4^{wt} or GFP-KIF4$^{520\text{-}1226}$ were treated as in Fig. 5 C and stained with anti CENP-T antibody. More than 50 kinetochore pairs were measured per cell line. D- and P-values were obtained by KS test. Compared with KIF4^{ON}, D = 0.58, P < 0.001 (KIF4^{OFF}); D = 0.30, P = 0.01 (GFP-KIF4^{wt}); and D = 0.49, P < 0.001 (GFP-KIF4$^{520\text{-}1226}$). Compared with KIF4^{OFF}, D = 0.26, P = 0.058 (GFP-KIF4$^{520\text{-}1226}$). Data are shown from a single representative experiment out of two repeats. (D) Intrinsic metaphase structure assay. KIF4$^{ON/OFF}$ cells or KIF4^{OFF} cells expressing GFP-KIF4^{wt} or GFP-KIF4$^{520\text{-}1226}$ were treated as for Fig. 5 E. 100 cells were scored for each cell line. Data are shown from a single representative experiment out of two repeats.

monitors the proper formation of a network of interactions between the nonhistone proteins and chromatin of mitotic chromosomes. Importantly, cohesin, the chromosomal passenger complex, and topo IIα are not required for a normal intrinsic metaphase structure of mitotic chromosomes (Vagnarelli et al., 2004; Spence et al., 2007), suggesting that the assay is not sensitive to general perturbations of chromosome structure.

We were surprised to find that the KIF4 N-terminal motor domain is required for its chromosomal functions. A KIF4 mutant lacking the motor domain binds to chromosomes but cannot rescue the elasticity (compliance) of centromeric heterochromatin or the intrinsic metaphase structure of KIF4-depleted chromosomes. It is unclear how classical kinesin motor activity would contribute to the chromosomal functions of KIF4, but this domain could interact with key partner proteins during chromosome formation.

In a previous RNAi study, KIF4 depletion was reported to cause chromosome hypercondensation in HeLa cells (Mazumdar et al., 2004). Mitotic chromosome morphology is exquisitely sensitive to time spent in mitosis and to the experimental treatment of cells during specimen preparation. Our data suggest that the loss of KIF4 does not dramatically alter the condensation of chicken chromosomes maintained under isotonic conditions; however, it does have a profound effect on their underlying structural integrity.

KIF4 and condensin can bind to one another (Geiman et al., 2004; Mazumdar et al., 2004), and depletion of either causes levels of the other to fall on isolated chromosomes. Double depletion of condensin and KIF4 yields a phenotype more severe than seen with either single depletion, essentially abolishing the formation of morphologically distinct mitotic chromosomes when cells are briefly treated with hypotonic solution before fixation. We therefore postulate that the two act in parallel or additive sequential pathways during chromosome formation (Fig. 9 d). Interestingly, the nuclear matrix protein DEK (Takata et al., 2009), which is significantly decreased in chromosomes depleted of KIF4, can induce positive supercoiling in closed circular DNA (Waldmann et al., 2002). The combination of KIF4 and DEK could potentially act in parallel with condensin to promote mitotic chromosome condensation.

It has been suggested that condensin functions catalytically to compact mitotic chromatin, and that the 5% remaining in chromosomes isolated from SMC2-KO cells (Ohta et al., 2010a) might be sufficient to support mitotic chromosome formation (Baxter and Aragón, 2012). According to that suggestion, KIF4 and condensin might function in the same pathway and the further approximately twofold drop in condensin levels after KIF4 depletion could cause condensin activity to fall below a threshold level required for mitotic chromosome formation.

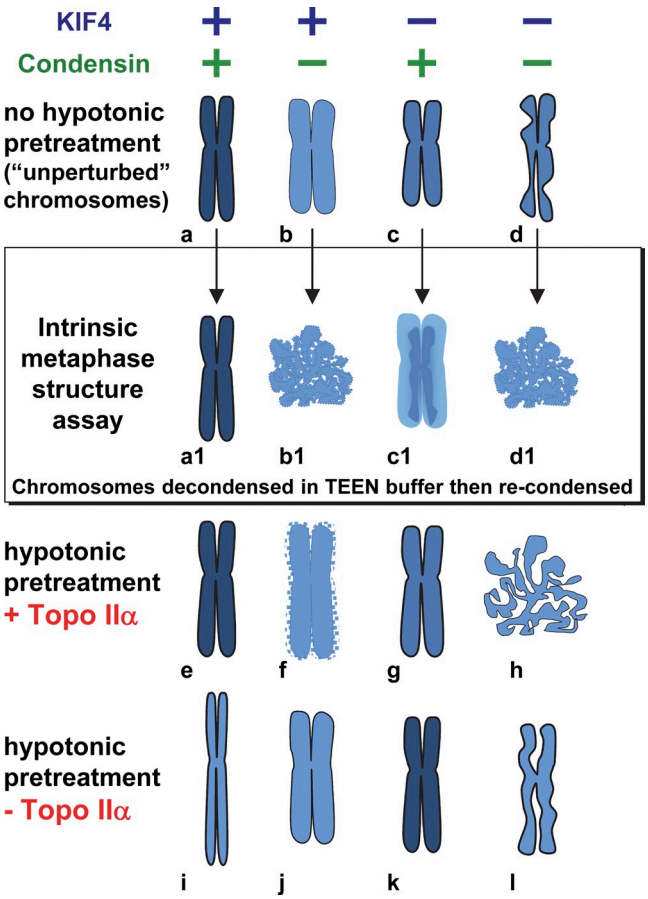

Figure 9. **Morphological and structural consequences of depleting condensin, KIF4, and topo IIα on mitotic chromosomes.** Shaping of mitotic chromosomes requires coordinated action of KIF4, condensins, and topo IIα. KIF4 and SMC2 are required for lateral compaction, whereas topo IIα is required for axial shortening. (a–d) Chromosomes prepared under the most "native" conditions consistent with visualization of individual chromosomes showed relatively minor perturbations after depletion of condensin or KIF4, but were significantly defective in the intrinsic metaphase structure assay. The morphological defects became more apparent when chromosomes were treated in hypotonic buffer (e–l).

Here, we tested that hypothesis by RNAi knockdown of CAP-H or CAP-D3 in SMC2-KO cells in order to lower condensin levels further. Neither treatment caused a significant further loss of chromosome morphology. Thus, another explanation is required for the observation that condensin depletion from *Xenopus* egg extracts results in a complete loss of mitotic chromosome formation (Hirano et al., 1997). Indeed, 2–5% of condensin typically remains in those depleted extracts (Shintomi and Hirano, 2011) and much of this presumably accumulates on added chromatin. We suspect that other differences—e.g., the spectrum of posttranslational modifications on the stockpiled histones in *Xenopus* eggs—could explain the different responses to condensin depletion.

One striking result from our experiments is that topo IIα is essential for axial shortening and appears to act independently and in opposition to both KIF4 and condensin in shaping mitotic chromosomes. This fits with previous studies, which found that topo IIα and condensin appear to have opposite activities in regulating centromere chromatin compliance (Spence et al., 2007; Ribeiro et al., 2009), and is consistent with a recent study in which budding yeast topo II was found to be particularly efficient at decatenating positively supercoiled DNA produced by condensin (Baxter et al., 2011). It was later suggested that topo II and condensin work both together and in opposition during chromosome condensation (Baxter and Aragón, 2012). Our data provide the first experimental evidence supporting this hypothesis.

Mitotic chromosomes formed in condensin-depleted cells appear to fall apart at anaphase onset in a process that requires the targeting of Repo-Man:PP1 to anaphase chromatin (Vagnarelli et al., 2006). If PP1 targeting is prevented at that time, sister chromatids lacking condensin I and II segregate with a near-normal condensed morphology. This observation suggested the existence of an additional chromatin condensation activity that we termed the regulator of chromosome architecture (RCA; Vagnarelli et al., 2006). Importantly, we do not think that KIF4 is RCA because recognizable chromosomes can form in cells depleted of both KIF4 and condensin. More recently, we found that Repo-Man interacts with histone H2B (Vagnarelli et al., 2011). It is therefore possible that histone remodeling and modification activities contribute to RCA activity. Indeed, RCA may correspond to the action of one or more factors that establish a combination of histone post-translational modifications and promote generalized chromatin condensation throughout mitosis. The PMM mark—H3T3-phK4me3R8me2 (Markaki et al., 2009)—could be one aspect of this mitotic chromatin "signature." Nonhistone factors, including KIF4, condensin, and topo IIα may then act to refine and shape the resulting structures.

Structural changes arising from the depletion of condensin and KIF4 are difficult to detect in chromosomes prepared under isotonic conditions designed to optimize their structural preservation (Fig. 9, a–d). However, mild hypotonic treatment of cells before fixation (Fig. 9, e–l) or use of our IMS assay (Fig. 9, a1–d1) renders the structural defects readily apparent.

When topo IIα is depleted, condensin continues to supercoil and "reel in" chromatin loops while KIF4 continues to cluster loops together. However, because strand passage is impaired, chromatid axes are prevented from shortening maximally, possibly because DNA strand passage might be required for chromosomes to counter the entropic repulsion of chromatin loops (Heermann, 2011). The result is longer, thinner chromosomes (Fig. 9 i; Uemura et al., 1987; Spence et al., 2007). When condensin or KIF4 are individually depleted, loops may be less supercoiled or clustered. Because chromatin compaction continues, possibly driven by RCA, chromosomes become shorter and wider (Fig. 9, b, c, f, and g). If KIF4 and topo IIα are simultaneously depleted, the chromatin compaction continues, but chromatid axes are prevented from shortening maximally. Overall, chromosomes attain a normal appearance (Fig. 9 k). If condensin is depleted, lateral compaction is impaired and chromatids adopt a "ragged" appearance after hypotonic swelling of cells (Fig. 9 f). Simultaneous depletion of condensin and topo II rescues this appearance, and the chromosomes appear swollen, but smooth (Fig. 9 j). If condensin and KIF4 are both depleted, chromatin condensation continues and we hypothesize that random strand passage by topo IIα causes the chromatin to form a disordered mass lacking recognizable chromosome morphology (Fig. 9, d and h). Simultaneous depletion of condensin,

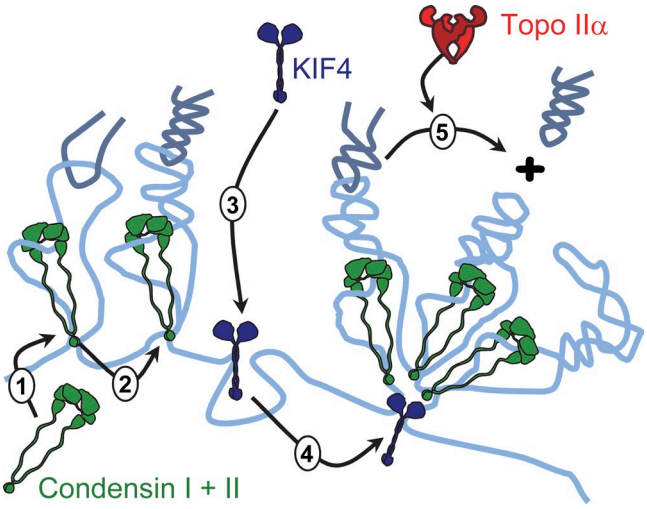

Figure 10. **Interplay between KIF4, condensin, and topo IIα in shaping mitotic chromosomes.** A model for interactions between KIF4, condensin, and topo IIα during mitotic chromosome formation.

KIF4, and topo IIα partially rescues the morphology, and individual chromosomes remain separate as the chromatin condenses (Fig. 9 l).

Because KIF4 is a dimeric molecule that binds both DNA and chromatin, our work suggests a model for the interplay between condensin, KIF4, and topo IIα during mitotic chromosome condensation in DT40 cells (Fig. 10). This model incorporates our earlier estimates that chromosomes have one KIF4 dimer per 340 kb of chromosomal DNA, one condensin complex per 90 kb, and one topo IIα dimer per 30 kb (Ohta et al., 2010a) as well as classical estimates of an average chromatin loop size of ∼80–100 kb in mitotic chromosomes (Earnshaw and Laemmli, 1983; Pienta and Coffey, 1984).

We propose that condensin binds to chromatin, forming loops that it then compacts by supercoiling (Fig. 10, part 1 and 2). KIF4 also independently binds to DNA, possibly forming higher-order loops and promoting their supercoiling by DEK and/or interactions with condensin (Fig. 10, part 3 and 4). Thus, condensin and KIF4 independently and additively contribute to lateral chromatid compaction. Lastly, topo IIα decatenates the loops in a step required for axial shortening (Fig. 10, part 5).

Our data suggest that even though isolated chromosomes contain >4,000 proteins (Ohta et al., 2010a), only a handful of these are directly involved in shaping the chromosomes. Although we now know much more about the interplay between the major chromosome nonhistone proteins during mitotic chromosome formation, this classical problem remains as mysterious and appealing as ever.

Materials and methods

Cell culture, transfections, and siRNA

The chicken lymphoma B cell line DT40 was cultured in RPMI 1640 medium containing 10% fetal bovine serum, 1% chicken serum, and penicillin/streptomycin at 39°C in 5% CO_2 in air as described previously (Takeda et al., 1992). The KIF4, SMC2, CAP-H, and CAP-D3 conditional knockouts were established previously as briefly described below (Hudson et al., 2003; Samejima et al., 2008; Green et al., 2012).

KIF4 KO: 2.3 kb 5′ and 4.0 kb 3′ genomic homology arms for KIF4 targeting vector were obtained from a lambda Fix II DT40 genomic library and cloned into the pTre-tight–based vector containing a puromycin resistance cassette. Correct targeting resulted in the deletion of a 7,463-bp untranslated region upstream of the ATG. ^{KIF4}tTA2 was transfected into heterozygotes in order to rescue KIF4 function in a conditional manner (shut off by addition of doxycycline; Samejima et. al, 2008).

SMC2 KO: 3 kb 5′ and 4.1 kb 3′ genomic homology arms for the SMC2 targeting vector were obtained from a lambda Fix II DT40 genomic library and cloned into a pBluescript-based vector that contained a histidinol resistance cassette. Correct targeting resulted in the deletion of 642 bp of the coding region downstream of the ATG. The SMC2 cDNA was obtained by RT-PCR using DT40 cell RNA as a template. Before gene targeting, the cDNA was cloned into pUHD 10.3 vector and cotransfected with ^{CMV}tTA3 in order to rescue SMC2 function in a conditional manner.

CAP-H KO: 2.6 kb 5′ and 4.2 kb 3′ genomic homology arms for the CAP-H targeting vector were amplified by PCR and cloned into a pBluescript based vector that contained either a puromycin or hygromycin resistance cassette. Correct targeting resulted in the deletion of 1,265 bp of the coding region downstream of the ATG. The CAP-H cDNA was obtained by RT-PCR using DT40 cell RNA as a template. This cDNA was cloned into the pUHD 10.3 vector and cotransfected with ^{CMV}tTA3 in order to rescue CAP-H function in a conditional manner.

CAP-D3 KO: 2.7 kb 5′ and 3.8 kb 3′ genomic homology arms for the CAP-D3 targeting vector were amplified by PCR and cloned into pBluescript-based vectors containing either a puromycin, histidinol, or hygromycin resistance cassette. Correct targeting resulted in the deletion of 630 bp from the coding region leaving 567 bp of the translated regions. The CAP-D3 cDNA was obtained by RT-PCR using DT40 cells RNA as a template. The cDNA was cloned into pUHD 10.3 vector and cotransfected with ^{SCII}tTA3 in order to rescue CAP-D3 function in a conditional manner (Samejima et. al, 2008).

The topo IIα inducible-shRNA cell line was reestablished in our laboratory as described previously (Johnson et al., 2009). In brief, a TetR expression construct (pcDNA3/TR; Invitrogen) and a vector containing H1/2×$TetO_2$ promoter:shtopo 2 cassette between HS4 insulator sequences were introduced into DT40 wild-type cells.

KIF4 knockouts expressing CENP-H–GFP were established using a CENP-H–GFP knock-in construct (hygromycin resistant) kindly provided by Y. Takami (University of Miyazaki, Miyazaki-shi, Japan). The SMC2 knockout cell line carrying lacO:lacI-GFP in which a construct containing 256 copies of the lac operator was introduced into cells was described elsewhere (Vagnarelli et al., 2006). The lac I array was detected with lac repressor (lac I)–GFP. KIF4 knockouts carrying a LacO:lacI-GFP were established as above (Vagnarelli et al., 2006). CAP-H knockout cell lines expressing CAP-H-GFP-TrAP; CAP-D3 knockouts expressing CAP-D3-GFP-TrAP; SMC2 knockouts expressing SMC2-GFP-STS or SMC2-TrAP; and KIF4 knockouts expressing GFP-$KIF4^{wt}$ or GFP-$KIF4^{510\text{-}1226}$ were established using corresponding cell lines and constructs. In each case, the corresponding cDNA obtained from DT40 cell RNA was cloned into original or modified pEGFPC1/N1 vectors from Takara Bio Inc. (Hudson et al., 2003; Samejima et al., 2008; Green et al., 2012). The TrAP tag contains $Histidine^6$, Streptavidin-binding peptide (SBP), and the S-tag (Hudson et al., 2008; Samejima et al., 2008). The STS tag contains SBP, a TEV protease cleavage site, and the S-tag, and was kindly donated by P. Kalitsis (Murdoch Childrens Research Institute, Royal Children's Hospital Melbourne, Australia).

Transfection to obtain stable cell lines was performed as described previously (Samejima et al., 2008). Transient transfection of either plasmid DNA or siRNA oligonucleotides was performed using Neon (Invitrogen). Typically 4 million cells were suspended in 100 µl buffer R. Either 4–8 µg of plasmid DNA or 2 µl of 100 µM siRNA oligonucleotides was added to the cell suspension and electroporated using setting 5. Sequences of siRNA oligonucleotides were: KIF4 (GGAUCSUUGUGACAGAACA, UGUUCUGUCACAAUGAUCC), topo IIα (GGAGUUGGUCCUGUUCUCA, UGAGAACAGGACCAACUCC), SMC2 (CAAAUAAGAAGAAGAUUUUTT, AAAAUCUUCUUCUUAUUUGTT), CAP-H (CAACAGGGUUCAACCUUAtt, UAAGGUUGAACCCUGUUUGgt), and CAP-D3 (GCACUGGCUGAAGGAGUUUtt, AAACUCCUUCAGCCAGUGCtt). All are shown in the orientation 5′ to 3′. Control oligonucleotide (AllStars Negative Control siRNA) was purchased from QIAGEN.

Subcloning, antibodies, and drug treatments

KIF4 cDNA digested with SacII/T4 DNA polymerase and KpnI was cloned into EGFPC1 (Takara Bio Inc.) digested with BglII/T4 DNA polymerase and KpnI to obtain GFP-$KIF4^{wt}$. GFP-$KIF4^{wt}$ was digested with the enzyme shown

within brackets below, blunted, and religated to obtain the corresponding constructs: GFP-KIF4$^{1\text{-}511}$ (BstEII–XhoI), GFP-KIF4$^{1\text{-}921}$ (EcoRI–XhoI), GFP-KIF4$^{510\text{-}1226}$ (SalI–BstEII), and GFP-KIF4$^{920\text{-}1226}$ (SalI–XhoI).

Antibodies used for immunoblotting and indirect immunofluorescence analysis were: rabbit anti-KIF4 (1:500), rabbit anti-SMC2 (1:300; Saitoh et al., 1994), mouse anti-SBP (1:250; Samejima et al., 2008), guinea pig anti-topo IIα (1:1,000; Earnshaw et al., 1985), mouse anti-tubulin B512 (1:4,000; Sigma-Aldrich), and rabbit anti–CENP-T (1:1,000; Hori et al., 2008).

Colcemid was added to a final concentration of 0.1 µg/ml (Invitrogen). MG132 (EMD Millipore) was added to a final concentration of 20 µM. Doxycycline (BD) was used at 0.5 µg/ml.

Measurement of interkinetochore distance and distance between sister chromatids

Cells were briefly (2–3 h) treated with either MG132 or colcemid and fixed in 4% paraformaldehyde (PFA)/PBS. Coverslips were mounted with Vectashield (Vector Laboratories) containing DAPI. For CENP-T staining, fixed cells were permeabilized with 0.15% Triton X-100 for 2 min and blocked with 1% BSA/PBS. Anti–CENP-T antibody (1:1,000 in blocking buffer) and anti–rabbit secondary antibody (Alexa Fluor 594, 1:1,000; Molecular Probes) were used to visualize kinetochore positions. 3D datasets were acquired using a cooled CCD camera (CoolSNAP HQ; Photometrics) on a wide-field microscope (DeltaVision RT; Applied Precision) with a 100× NA 1.4 Plan Apochromat lens. The datasets were deconvolved with softWoRx (Applied Precision). Apart from FRAP, the acquisition of images was performed as above throughout this study. Distances between paired kinetochores or LacO/LacI-GFP spots were measured using softWoRx only when they were in the same focal plane.

Microscopy of mitotic chromosomes—general note

Because chromosomes are highly charged polymers, they are exquisitely sensitive to changes in ionic conditions both in vivo and in vitro. This was examined in detail and discussed in Earnshaw and Laemmli (1983). For example, the hypotonic treatment of cells that enabled Tjio and Levan (1956) to visualize individual chromosomes and determine the human chromosome number somehow stresses the chromosome structure even though it is performed on living cells. This can be seen clearly in Fig. 7 A. This treatment can be informative—we found it to be absolutely necessary to obtain spreads where we could measure the chromosome length with confidence—but it can also influence measurements of chromosome dimensions. Where possible, we have avoided the use of hypotonic treatments and have "fixed" chromosomes with methanol/acetic acid. This is not a chemical fixation in the traditional sense, and probably works by precipitating chromosomal proteins in situ. Chromosomes treated in this way tend to have much sharper outlines than chromosomes fixed with formaldehyde or glutaraldehyde, and indeed chromosomes can still swell and shrink dramatically after extensive glutaraldehyde fixation (Earnshaw and Laemmli, 1983). The important thing is that comparisons between chromosomes depleted of different proteins are made under identical preparation conditions and ideally in the same experiment. For details of the processing of each sample, see Table S1. Fig. 9 summarizes the chromosome morphologies after various treatments.

Indirect immunofluorescence of chromosome spreads

Cells were briefly (2–3 h) treated with colcemid, hypotonically swollen in 75 mM KCl, fixed in ice-cold methanol/acetic acid, and dropped on slides to obtain chromosome spreads. The chromosome spreads were stained with first antibodies (guinea pig anti-topo IIα, mouse anti-SBP, and rabbit anti-KIF4) in TEEN buffer, washed with KB buffer, and then stained with secondary antibodies (Alexa Fluor 488, 1:500; Alexa Fluor 594, 1:1,000; from Molecular Probes). 3D datasets were acquired and processed as above. The datasets were converted to Quick Projections in softWoRx, exported as TIFF files, and imported into Adobe Photoshop for final presentation.

Intrinsic metaphase structure (IMS) assay

Cells were incubated with colcemid at 0.1 µg/ml for 6–12 h, then allowed to attach to polylysine-coated slides for 30 min to 1 h before the assay. Cells were treated with two cycles of TEEN buffer (1 mM triethanolamine/HCl, pH 8.5, 0.2 mM NaEDTA, and 25 mM NaCl) and RSB buffer (10 mM Tris/HCl, pH 7.4, 10 mM NaCl, and 5 mM $MgCl_2$) and fixed with 4% PFA in the corresponding buffers.

Quantification of SMC2-GFP signal

SMC2^{OFF} cells expressing SMC2-GFP-STS were transfected with either KIF4 or control siRNA oligonucleotides. After 20–24 h, cells were fixed with PFA/PBS and stained with anti–CENP-T antibody and DAPI. 3D datasets of 11 sections were acquired and deconvolved with softWoRx. Mean intensity was measured in a 0.19-µm^2 area at five kinetochores, five chromosome arms, and five cytosolic regions in each of 20 maximum-projected prometaphase cells using Image-Pro Plus 7.0 (Media Cybernetics). Values for kinetochores and chromosome arms were normalized against those obtained for cytosol.

FRAP

Experiments were performed on a laser-scanning confocal microscope (model SP5; Leica) using a 488-nm laser and a 63×, 1.4 NA objective lens. Chicken DT40 cells cultured in Leibovitz's L-15 media (Gibco) supplemented with 10% FBS and 1% chicken serum were imaged at 37°C in a heated chamber and gassed using 5% CO_2 in air. Five prebleach images were taken followed by bleaching a region of the chromosome for 0.4–0.8 s at 100% laser intensity so that between 20 and 40% fluorescence intensity was retained. Fluorescence recovery was measured every 0.4 s. Images were processed with Image-Pro Plus 7.0. The resulting intensity measurements were corrected for photobleaching and normalized according to Phair and Misteli (2001). In brief, a circular region of interest (0.75, 1 or 2 µm in diameter) was applied to each frame in the FRAP sequence. This region included the cytosol, the bleached chromosome area, the nonbleached chromosome area, and the extracellular milieu. This allowed us to automatically correct the data for photobleaching compared with five prebleach images. Movement of the bleached area due to cell/chromosome movement was relatively minor, and was corrected manually. The $t_{1/2}$ values were calculated from the fluorescence values after normalization. The first post-bleach value was set to zero and the mean of the final 10 points of the fluorescence recovery curves was set to 100.

Quantitative immunoblotting

Membranes were incubated with the relevant primary antibodies recognizing α-tubulin, KIF4, SMC2, topo IIα, and GFP, then subsequently with IRDye-labeled secondary antibodies (LI-COR Biosciences). Fluorescence intensities were subsequently determined using a CCD scanner (Odyssey; LI-COR Biosciences) according to the manufacturer's instructions.

SILAC-labeled mitotic chromosome isolation and analysis

For labeling of lysine and arginine by carbon 13 and nitrogen 15, cells were maintained in RPMI without L-lysine and L-arginine (Thermo Fisher Scientific) supplemented with 10% (vol/vol) FBS dialyzed 10,000 molecular weight cut-off (Sigma-Aldrich) and containing 100 µg/ml U-$^{13}C_6{}^{15}N_2$-L-lysine:2HCl plus 30 µg/ml U-$^{13}C_6{}^{15}N_4$-L-arginine:HCl (Sigma-Aldrich). To enrich mitotic cells, DT40 cells were incubated with nocodazole for 13 h, resulting in a mitotic index of 70–90%. Mitotic chromosomes were isolated using the polyamine-EDTA buffer system as optimized for chicken DT40 cells (Lewis and Laemmli, 1982; Ohta et al., 2010a). Proteins were separated into a high and a low molecular weight fraction by SDS-PAGE, in-gel digested using trypsin (Shevchenko et al., 2006), and fractionated into 30 fractions each using SCX. The individual SCX fractions were desalted using StageTips (Rappsilber et al., 2003) and analyzed using LC-MS on a mass spectrometer (LTQ-Orbitrap Velos; Thermo Fisher Scientific) coupled to HPLC via a nanoelectrospray ion source. The 20 most intense ions of a full MS acquired in the Orbitrap analyzer were fragmented and analyzed in the linear ion trap. The MS data were analyzed using MaxQuant version 1.1.1.36 (Cox and Mann, 2008) and the IPI.Chick.v3.75 database. For more details, see the extended experimental procedures in Ohta et al. (2010a).

Online supplemental material

Fig. S1 shows the quantitation of KIF4 depletions and further explores the effect of SMC2 depletion on KIF4 localization. Fig. S2 shows further controls for FRAP experiments. Fig. S3 further characterizes the chromosomal phenotypes following KIF4 depletion. Fig. S4 provides further evidence that the chromosomal functions of KIF4 require its motor domain. Table S1 provides detailed information on the exact cell pretreatment and fixation conditions for all micrographs. Online supplemental material is available at http://www.jcb.org/cgi/content/full/jcb.201202155/DC1.

This work was funded by The Wellcome Trust, of which W.C. Earnshaw is a Principal Research Fellow [grant number 073915] and J. Rappsilber is a Senior Research Fellow [grant number 084229]. The Wellcome Trust Centre for Cell Biology is supported by core grant numbers 077707 and 092076, and the work was also supported by Wellcome Trust instrument grant 091020.

Submitted: 29 February 2012
Accepted: 17 October 2012

References

Adolph, K.W., S.M. Cheng, and U.K. Laemmli. 1977a. Role of nonhistone proteins in metaphase chromosome structure. *Cell*. 12:805–816. http://dx.doi.org/10.1016/0092-8674(77)90279-3

Adolph, K.W., S.M. Cheng, J.R. Paulson, and U.K. Laemmli. 1977b. Isolation of a protein scaffold from mitotic HeLa cell chromosomes. *Proc. Natl. Acad. Sci. USA*. 11:4937–4941. http://dx.doi.org/10.1073/pnas.74.11.4937

Aizawa, H., Y. Sekine, R. Takemura, Z. Zhang, M. Nangaku, and N. Hirokawa. 1992. Kinesin family in murine central nervous system. *J. Cell Biol.* 119:1287–1296. http://dx.doi.org/10.1083/jcb.119.5.1287

Baxter, J., and L. Aragón. 2012. A model for chromosome condensation based on the interplay between condensin and topoisomerase II. *Trends Genet.* 28:110–117. http://dx.doi.org/10.1016/j.tig.2011.11.004

Baxter, J., N. Sen, V.L. Martínez, M.E. De Carandini, J.B. Schvartzman, J.F. Diffley, and L. Aragón. 2011. Positive supercoiling of mitotic DNA drives decatenation by topoisomerase II in eukaryotes. *Science*. 331:1328–1332. http://dx.doi.org/10.1126/science.1201538

Belmont, A.S. 2006. Mitotic chromosome structure and condensation. *Curr. Opin. Cell Biol.* 18:632–638. http://dx.doi.org/10.1016/j.ceb.2006.09.007

Bhat, M.A., A.V. Philp, D.M. Glover, and H.J. Bellen. 1996. Chromatid segregation at anaphase requires the barren product, a novel chromosome-associated protein that interacts with Topoisomerase II. *Cell*. 87:1103–1114. http://dx.doi.org/10.1016/S0092-8674(00)81804-8

Bouck, D.C., and K. Bloom. 2007. Pericentric chromatin is an elastic component of the mitotic spindle. *Curr. Biol.* 17:741–748. http://dx.doi.org/10.1016/j.cub.2007.03.033

Carpenter, A.J., and A.C. Porter. 2004. Construction, characterization, and complementation of a conditional-lethal DNA topoisomerase IIalpha mutant human cell line. *Mol. Biol. Cell*. 15:5700–5711. http://dx.doi.org/10.1091/mbc.E04-08-0732

Castoldi, M., and I. Vernos. 2006. Chromokinesin Xklp1 contributes to the regulation of microtubule density and organization during spindle assembly. *Mol. Biol. Cell*. 17:1451–1460. http://dx.doi.org/10.1091/mbc.E05-04-0271

Chang, C.J., S. Goulding, W.C. Earnshaw, and M. Carmena. 2003. RNAi analysis reveals an unexpected role for topoisomerase II in chromosome arm congression to a metaphase plate. *J. Cell Sci.* 116:4715–4726. http://dx.doi.org/10.1242/jcs.00797

Christensen, M.O., M.K. Larsen, H.U. Barthelmes, R. Hock, C.L. Andersen, E. Kjeldsen, B.R. Knudsen, O. Westergaard, F. Boege, and C. Mielke. 2002. Dynamics of human DNA topoisomerases IIalpha and IIbeta in living cells. *J. Cell Biol.* 157:31–44. http://dx.doi.org/10.1083/jcb.200112023

Cox, J., and M. Mann. 2008. MaxQuant enables high peptide identification rates, individualized p.p.b.-range mass accuracies and proteome-wide protein quantification. *Nat. Biotechnol.* 26:1367–1372. http://dx.doi.org/10.1038/nbt.1511

Csankovszki, G., K. Collette, K. Spahl, J. Carey, M. Snyder, E. Petty, U. Patel, T. Tabuchi, H. Liu, I. McLeod, et al. 2009. Three distinct condensin complexes control *C. elegans* chromosome dynamics. *Curr. Biol.* 19:9–19. http://dx.doi.org/10.1016/j.cub.2008.12.006

Earnshaw, W.C., and M.M.S. Heck. 1985. Localization of topoisomerase II in mitotic chromosomes. *J. Cell Biol.* 100:1716–1725. http://dx.doi.org/10.1083/jcb.100.5.1716

Earnshaw, W.C., and U.K. Laemmli. 1983. Architecture of metaphase chromosomes and chromosome scaffolds. *J. Cell Biol.* 96:84–93. http://dx.doi.org/10.1083/jcb.96.1.84

Earnshaw, W.C., B. Halligan, C.A. Cooke, M.M.S. Heck, and L.F. Liu. 1985. Topoisomerase II is a structural component of mitotic chromosome scaffolds. *J. Cell Biol.* 100:1706–1715. http://dx.doi.org/10.1083/jcb.100.5.1706

Gasser, S.M., T. Laroche, J. Falquet, E. Boy de la Tour, and U.K. Laemmli. 1986. Metaphase chromosome structure. Involvement of topoisomerase II. *J. Mol. Biol.* 188:613–629. http://dx.doi.org/10.1016/S0022-2836(86)80010-9

Geiman, T.M., U.T. Sankpal, A.K. Robertson, Y. Chen, M. Mazumdar, J.T. Heale, J.A. Schmiesing, W. Kim, K. Yokomori, Y. Zhao, and K.D. Robertson. 2004. Isolation and characterization of a novel DNA methyltransferase complex linking DNMT3B with components of the mitotic chromosome condensation machinery. *Nucleic Acids Res.* 32:2716–2729. http://dx.doi.org/10.1093/nar/gkh589

Gerlich, D., T. Hirota, B. Koch, J.M. Peters, and J. Ellenberg. 2006. Condensin I stabilizes chromosomes mechanically through a dynamic interaction in live cells. *Curr. Biol.* 16:333–344. http://dx.doi.org/10.1016/j.cub.2005.12.040

Gonzalez, R.E., C.U. Lim, K. Cole, C.H. Bianchini, G.P. Schools, B.E. Davis, I. Wada, I.B. Roninson, and E.V. Broude. 2011. Effects of conditional depletion of topoisomerase II on cell cycle progression in mammalian cells. *Cell Cycle*. 10:3505–3514. http://dx.doi.org/10.4161/cc.10.20.17778

Green, L.C., P. Kalitsis, T.M. Chang, M. Cipetic, J.-H. Kim, O. Marshall, L. Turnbull, C.B. Whitchurch, P. Vagnarelli, K. Samejima, et al. 2012. Contrasting roles of condensin I and condensin II in mitotic chromosome formation. *J. Cell Sci.* 125:1591–1604. http://dx.doi.org/10.1242/jcs.097790

Hagstrom, K.A., V.F. Holmes, N.R. Cozzarelli, and B.J. Meyer. 2002. *C. elegans* condensin promotes mitotic chromosome architecture, centromere organization, and sister chromatid segregation during mitosis and meiosis. *Genes Dev.* 16:729–742. http://dx.doi.org/10.1101/gad.968302

Heermann, D.W. 2011. Physical nuclear organization: loops and entropy. *Curr. Opin. Cell Biol.* 23:332–337. http://dx.doi.org/10.1016/j.ceb.2011.03.010

Hirano, T., and T.J. Mitchison. 1994. A heterodimeric coiled-coil protein required for mitotic chromosome condensation in vitro. *Cell*. 79:449–458. http://dx.doi.org/10.1016/0092-8674(94)90254-2

Hirano, T., R. Kobayashi, and M. Hirano. 1997. Condensins, chromosome condensation protein complexes containing XCAP-C, XCAP-E and a *Xenopus* homolog of the *Drosophila* Barren protein. *Cell*. 89:511–521. http://dx.doi.org/10.1016/S0092-8674(00)80233-0

Holm, C., T. Goto, J.C. Wang, and D. Botstein. 1985. DNA topoisomerase II is required at the time of mitosis in yeast. *Cell*. 41:553–563. http://dx.doi.org/10.1016/S0092-8674(85)80028-3

Hori, T., M. Amano, A. Suzuki, C.B. Backer, J.P. Welburn, Y. Dong, B.F. McEwen, W.H. Shang, E. Suzuki, K. Okawa, et al. 2008. CCAN makes multiple contacts with centromeric DNA to provide distinct pathways to the outer kinetochore. *Cell*. 135:1039–1052. http://dx.doi.org/10.1016/j.cell.2008.10.019

Hu, C.K., M. Coughlin, C.M. Field, and T.J. Mitchison. 2011. KIF4 regulates midzone length during cytokinesis. *Curr. Biol.* 21:815–824. http://dx.doi.org/10.1016/j.cub.2011.04.019

Hudson, D.F., P. Vagnarelli, R. Gassmann, and W.C. Earnshaw. 2003. Condensin is required for nonhistone protein assembly and structural integrity of vertebrate mitotic chromosomes. *Dev. Cell*. 5:323–336. http://dx.doi.org/10.1016/S1534-5807(03)00199-0

Hudson, D.F., S. Ohta, T. Freisinger, F. Macisaac, L. Sennels, F. Alves, F. Lai, A. Kerr, J. Rappsilber, and W.C. Earnshaw. 2008. Molecular and genetic analysis of condensin function in vertebrate cells. *Mol. Biol. Cell*. 19:3070–3079. http://dx.doi.org/10.1091/mbc.E08-01-0057

Hudson, D.F., K.M. Marshall, and W.C. Earnshaw. 2009. Condensin: Architect of mitotic chromosomes. *Chromosome Res.* 17:131–144. http://dx.doi.org/10.1007/s10577-008-9009-7

Jaqaman, K., E.M. King, A.C. Amaro, J.R. Winter, J.F. Dorn, H.L. Elliott, N. McHedlishvili, S.E. McClelland, I.M. Porter, M. Posch, et al. 2010. Kinetochore alignment within the metaphase plate is regulated by centromere stiffness and microtubule depolymerases. *J. Cell Biol.* 188:665–679. http://dx.doi.org/10.1083/jcb.200909005

Johnson, M., H.H. Phua, S.C. Bennett, J.M. Spence, and C.J. Farr. 2009. Studying vertebrate topoisomerase 2 function using a conditional knockdown system in DT40 cells. *Nucleic Acids Res.* 37:e98. http://dx.doi.org/10.1093/nar/gkp480

Kaitna, S., P. Pasierbek, M. Jantsch, J. Loidl, and M. Glotzer. 2002. The aurora B kinase AIR-2 regulates kinetochores during mitosis and is required for separation of homologous chromosomes during meiosis. *Curr. Biol.* 12:798–812. http://dx.doi.org/10.1016/S0960-9822(02)00820-5

Kurasawa, Y., W.C. Earnshaw, Y. Mochizuki, N. Dohmae, and K. Todokoro. 2004. Essential roles of KIF4 and its binding partner PRC1 in organized central spindle midzone formation. *EMBO J.* 23:3237–3248. http://dx.doi.org/10.1038/sj.emboj.7600347

Kwon, M., S. Morales-Mulia, I. Brust-Mascher, G.C. Rogers, D.J. Sharp, and J.M. Scholey. 2004. The chromokinesin, KLP3A, dives mitotic spindle pole separation during prometaphase and anaphase and facilitates chromatid motility. *Mol. Biol. Cell*. 15:219–233. http://dx.doi.org/10.1091/mbc.E03-07-0489

Lee, Y.M., S. Lee, E. Lee, H. Shin, H. Hahn, W. Choi, and W. Kim. 2001. Human kinesin superfamily member 4 is dominantly localized in the nuclear matrix and is associated with chromosomes during mitosis. *Biochem. J.* 360:549–556. http://dx.doi.org/10.1042/0264-6021:3600549

Lewis, C.D., and U.K. Laemmli. 1982. Higher order metaphase chromosome structure: evidence for metalloprotein interactions. *Cell*. 29:171–181. http://dx.doi.org/10.1016/0092-8674(82)90101-5

MacCallum, D.E., A. Losada, R. Kobayashi, and T. Hirano. 2002. ISWI remodeling complexes in *Xenopus* egg extracts: identification as major chromosomal components that are regulated by INCENP-aurora B. *Mol. Biol. Cell*. 13:25–39. http://dx.doi.org/10.1091/mbc.01-09-0441

Maeshima, K., and U.K. Laemmli. 2003. A two-step scaffolding model for mitotic chromosome assembly. *Dev. Cell*. 4:467–480. http://dx.doi.org/10.1016/S1534-5807(03)00092-3

Markaki, Y., A. Christogianni, A.S. Politou, and S.D. Georgatos. 2009. Phosphorylation of histone H3 at Thr3 is part of a combinatorial pattern that marks and configures mitotic chromatin. *J. Cell Sci.* 122:2809–2819. http://dx.doi.org/10.1242/jcs.043810

Marko, J.F. 2008. Micromechanical studies of mitotic chromosomes. *Chromosome Res.* 16:469–497. http://dx.doi.org/10.1007/s10577-008-1233-7

Mazumdar, M., and T. Misteli. 2005. Chromokinesins: multitalented players in mitosis. *Trends Cell Biol.* 15:349–355. http://dx.doi.org/10.1016/j.tcb.2005.05.006

Mazumdar, M., S. Sundareshan, and T. Misteli. 2004. Human chromokinesin KIF4A functions in chromosome condensation and segregation. *J. Cell Biol.* 166:613–620. http://dx.doi.org/10.1083/jcb.200401142

Mazumdar, M., M.H. Sung, and T. Misteli. 2011. Chromatin maintenance by a molecular motor protein. *Nucleus*. 2:591–600. http://dx.doi.org/10.4161/nucl.2.6.18044

Midorikawa, R., Y. Takei, and N. Hirokawa. 2006. KIF4 motor regulates activity-dependent neuronal survival by suppressing PARP-1 enzymatic activity. *Cell*. 125:371–383. http://dx.doi.org/10.1016/j.cell.2006.02.039

Mora-Bermúdez, F., D. Gerlich, and J. Ellenberg. 2007. Maximal chromosome compaction occurs by axial shortening in anaphase and depends on Aurora kinase. *Nat. Cell Biol.* 9:822–831. http://dx.doi.org/10.1038/ncb1606

Moser, S.C., and J.R. Swedlow. 2011. How to be a mitotic chromosome. *Chromosome Res.* 19:307–319. http://dx.doi.org/10.1007/s10577-011-9198-3

Oh, S., H. Hahn, T.A. Torrey, H. Shin, W. Choi, Y.M. Lee, H.C. Morse, and W. Kim. 2000. Identification of the human homologue of mouse KIF4, a kinesin superfamily motor protein. *Biochim. Biophys. Acta*. 1493:219–224. http://dx.doi.org/10.1016/S0167-4781(00)00151-2

Ohta, S., J.C. Bukowski-Wills, L. Sanchez-Pulido, Fde.L. Alves, L. Wood, Z.A. Chen, M. Platani, L. Fischer, D.F. Hudson, C.P. Ponting, et al. 2010a. The protein composition of mitotic chromosomes determined using multiclassifier combinatorial proteomics. *Cell*. 142:810–821. http://dx.doi.org/10.1016/j.cell.2010.07.047

Ohta, S., J.C. Bukowski-Wills, L. Wood, F. de Lima Alves, Z. Chen, J. Rappsilber, and W.C. Earnshaw. 2010b. Proteomics of isolated mitotic chromosomes identifies the kinetochore protein Ska3/Rama1. *Cold Spring Harb. Symp. Quant. Biol.* 75:433–438. http://dx.doi.org/10.1101/sqb.2010.75.022

Ohta, S., L. Wood, J.C. Bukowski-Wills, J. Rappsilber, and W.C. Earnshaw. 2011. Building mitotic chromosomes. *Curr. Opin. Cell Biol.* 23:114–121. http://dx.doi.org/10.1016/j.ceb.2010.09.009

Oliveira, R.A., S. Heidmann, and C.E. Sunkel. 2007. Condensin I binds chromatin early in prophase and displays a highly dynamic association with *Drosophila* mitotic chromosomes. *Chromosoma*. 116:259–274. http://dx.doi.org/10.1007/s00412-007-0097-5

Ono, T., A. Losada, M. Hirano, M.P. Myers, A.F. Neuwald, and T. Hirano. 2003. Differential contributions of condensin I and condensin II to mitotic chromosome architecture in vertebrate cells. *Cell*. 115:109–121. http://dx.doi.org/10.1016/S0092-8674(03)00724-4

Phair, R.D., and T. Misteli. 2001. Kinetic modelling approaches to in vivo imaging. *Nat. Rev. Mol. Cell Biol.* 2:898–907. http://dx.doi.org/10.1038/35103000

Pienta, K.J., and D.S. Coffey. 1984. A structural analysis of the role of the nuclear matrix and DNA loops in the organization of the nucleus and chromosome. *J. Cell Sci. Suppl.* 1:123–135.

Rappsilber, J., Y. Ishihama, and M. Mann. 2003. Stop and go extraction tips for matrix-assisted laser desorption/ionization, nanoelectrospray, and LC/MS sample pretreatment in proteomics. *Anal. Chem.* 75:663–670. http://dx.doi.org/10.1021/ac026117i

Ribeiro, S.A., J.C. Gatlin, Y. Dong, A. Joglekar, L. Cameron, D.F. Hudson, C.J. Farr, B.F. McEwen, E.D. Salmon, W.C. Earnshaw, and P. Vagnarelli. 2009. Condensin regulates the stiffness of vertebrate centromeres. *Mol. Biol. Cell*. 20:2371–2380. http://dx.doi.org/10.1091/mbc.E08-11-1127

Saitoh, N., I.G. Goldberg, E.R. Wood, and W.C. Earnshaw. 1994. ScII: an abundant chromosome scaffold protein is a member of a family of putative ATPases with an unusual predicted tertiary structure. *J. Cell Biol.* 127:303–318. http://dx.doi.org/10.1083/jcb.127.2.303

Saka, Y., T. Sutani, Y. Yamashita, S. Saitoh, M. Takeuchi, Y. Nakaseko, and M. Yanagida. 1994. Fission yeast cut3 and cut14, members of a ubiquitous protein family, are required for chromosome condensation and segregation in mitosis. *EMBO J.* 13:4938–4952.

Sakaguchi, A., and A. Kikuchi. 2004. Functional compatibility between isoform alpha and beta of type II DNA topoisomerase. *J. Cell Sci.* 117:1047–1054. http://dx.doi.org/10.1242/jcs.00977

Samejima, K., H. Ogawa, C.A. Cooke, D.F. Hudson, F. Macisaac, S.A. Ribeiro, P. Vagnarelli, S. Cardinale, A. Kerr, F. Lai, et al. 2008. A promoter-hijack strategy for conditional shutdown of multiply spliced essential cell cycle genes. *Proc. Natl. Acad. Sci. USA*. 105:2457–2462. http://dx.doi.org/10.1073/pnas.0712083105

Sekine, Y., Y. Okada, Y. Noda, S. Kondo, H. Aizawa, R. Takemura, and N. Hirokawa. 1994. A novel microtubule-based motor protein (KIF4) for organelle transports, whose expression is regulated developmentally. *J. Cell Biol.* 127:187–201. http://dx.doi.org/10.1083/jcb.127.1.187

Shevchenko, A., H. Tomas, J. Havlis, J.V. Olsen, and M. Mann. 2006. In-gel digestion for mass spectrometric characterization of proteins and proteomes. *Nat. Protoc.* 1:2856–2860. http://dx.doi.org/10.1038/nprot.2006.468

Shintomi, K., and T. Hirano. 2011. The relative ratio of condensin I to II determines chromosome shapes. *Genes Dev.* 25:1464–1469. http://dx.doi.org/10.1101/gad.2060311

Spence, J.M., H.H. Phua, W. Mills, A.J. Carpenter, A.C. Porter, and C.J. Farr. 2007. Depletion of topoisomerase IIalpha leads to shortening of the metaphase interkinetochore distance and abnormal persistence of PICH-coated anaphase threads. *J. Cell Sci.* 120:3952–3964. http://dx.doi.org/10.1242/jcs.013730

Steffensen, S., P.A. Coelho, N. Cobbe, S. Vass, M. Costa, B. Hassan, S.N. Prokopenko, H. Bellen, M.M.S. Heck, and C.E. Sunkel. 2001. A role for *Drosophila* SMC4 in the resolution of sister chromatids in mitosis. *Curr. Biol.* 11:295–307. http://dx.doi.org/10.1016/S0960-9822(01)00096-3

Strunnikov, A.V., V.L. Larionov, and D. Koshland. 1993. *SMC1*: an essential yeast gene encoding a putative head-rod-tail protein is required for nuclear division and defines a new ubiquitous protein family. *J. Cell Biol.* 123:1635–1648. http://dx.doi.org/10.1083/jcb.123.6.1635

Takata, H., H. Nishijima, S. Ogura, T. Sakaguchi, P.A. Bubulya, T. Mochizuki, and K. Shibahara. 2009. Proteome analysis of human nuclear insoluble fractions. *Genes Cells*. 14:975–990. http://dx.doi.org/10.1111/j.1365-2443.2009.01324.x

Takeda, S., E.L. Masteller, C.B. Thompson, and J.M. Buerstedde. 1992. RAG-2 expression is not essential for chicken immunoglobulin gene conversion. *Proc. Natl. Acad. Sci. USA*. 89:4023–4027. http://dx.doi.org/10.1073/pnas.89.9.4023

Tavormina, P.A., M.G. Côme, J.R. Hudson, Y.Y. Mo, W.T. Beck, and G.J. Gorbsky. 2002. Rapid exchange of mammalian topoisomerase II alpha at kinetochores and chromosome arms in mitosis. *J. Cell Biol.* 158:23–29. http://dx.doi.org/10.1083/jcb.200202053

Tjio, J.H., and G. Levan. 1956. The chromosome number of man. *Hereditas*. 42:1–6. http://dx.doi.org/10.1111/j.1601-5223.1956.tb03010.x

Uemura, T., H. Ohkura, Y. Adachi, K. Morino, K. Shiozaki, and M. Yanagida. 1987. DNA topoisomerase II is required for condensation and separation of mitotic chromosomes in *S. pombe*. *Cell*. 50:917–925. http://dx.doi.org/10.1016/0092-8674(87)90518-6

Vagnarelli, P., C. Morrison, H. Dodson, E. Sonoda, S. Takeda, and W.C. Earnshaw. 2004. Analysis of Scc1-deficient cells defines a key metaphase role of vertebrate cohesin in linking sister kinetochores. *EMBO Rep.* 5:167–171. http://dx.doi.org/10.1038/sj.embor.7400077

Vagnarelli, P., D.F. Hudson, S.A. Ribeiro, L. Trinkle-Mulcahy, J.M. Spence, F. Lai, C.J. Farr, A.I. Lamond, and W.C. Earnshaw. 2006. Condensin and Repo-Man-PP1 co-operate in the regulation of chromosome architecture during mitosis. *Nat. Cell Biol.* 8:1133–1142. http://dx.doi.org/10.1038/ncb1475

Vagnarelli, P., S. Ribeiro, L. Sennels, L. Sanchez-Pulido, F. de Lima Alves, T. Verheyen, D.A. Kelly, C.P. Ponting, J. Rappsilber, and W.C. Earnshaw. 2011. Repo-Man coordinates chromosomal reorganization with nuclear envelope reassembly during mitotic exit. *Dev. Cell*. 21:328–342. http://dx.doi.org/10.1016/j.devcel.2011.06.020

Vernos, I., J. Raats, T. Hirano, J. Heasman, E. Karsenti, and C. Wylie. 1995. Xklp1, a chromosomal *Xenopus* kinesin-like protein essential for spindle organization and chromosome positioning. *Cell*. 81:117–127. http://dx.doi.org/10.1016/0092-8674(95)90376-3

Waldmann, T., C. Eckerich, M. Baack, and C. Gruss. 2002. The ubiquitous chromatin protein DEK alters the structure of DNA by introducing positive supercoils. *J. Biol. Chem.* 277:24988–24994. http://dx.doi.org/10.1074/jbc.M204045200

Wang, S.Z., and R. Adler. 1995. Chromokinesin: a DNA-binding, kinesin-like nuclear protein. *J. Cell Biol.* 128:761–768. http://dx.doi.org/10.1083/jcb.128.5.761

Williams, B.C., M.F. Riedy, E.V. Williams, M. Gatti, and M.L. Goldberg. 1995. The *Drosophila* kinesin-like protein KLP3A is a midbody component required for central spindle assembly and initiation of cytokinesis. *J. Cell Biol.* 129:709–723. http://dx.doi.org/10.1083/jcb.129.3.709

Wu, G., L. Zhou, L. Khidr, X.E. Guo, W. Kim, Y.M. Lee, T. Krasieva, and P.L. Chen. 2008. A novel role of the chromokinesin Kif4A in DNA damage response. *Cell Cycle*. 7:2013–2020. http://dx.doi.org/10.4161/cc.7.13.6130